Engineering metal-organic frameworks for adsorption-based gas separations: from process to atomic scale

Marco Taddei[a,] and Camille Petit[b,*]*

[a] Department of Chemistry and Industrial Chemistry, University of Pisa, Via Giuseppe Moruzzi, 13, 56124, Pisa, Italy. Email: marco.taddei@unipi.it

[b] Barrer Centre, Department of Chemical Engineering, Imperial College London, South Kensington Campus, London SW7 2AZ, UK. E-mail: camille.petit@imperial.ac.uk

ABSTRACT

Metal-organic frameworks (MOFs) are the object of intense research targeting their deployment as adsorbents for a wide range of gas separations, such as CO_2 capture, biogas upgrading, air separation and small hydrocarbons separation. The scope of this review is to provide chemists, material scientists and engineers with an overview of the state-of-the-art and of the main challenges in the field of adsorption-based gas separations using MOFs. To do so, we first discuss current gas separation challenges for which adsorption could play a role. The following three sections of the paper describe process-level considerations in the design, selection and deployment of MOFs as sorbents and subsequently focus on material-level considerations. Both the process and the material aspects cover experimental and computational work. Going from the process scale to the atomic scale, we aim to highlight the links and synergies between the two and identify the current barriers that hamper the development of adsorption-based gas separations using MOFs as sorbents. Throughout the article, we also provide fundamental and technical information related to MOFs design, synthesis, characterisation and sorption testing.

Design, System, Application

The sheer number of known MOFs and the virtually infinite number of potentially synthesisable MOFs make the endeavour of identifying a MOF sorbent with ideal features for a given gas separation process a particularly challenging one. A successful implementation of MOFs in this context must start from acknowledging the multiscale nature of the problem, calling for a cross-disciplinary effort that requires the combined expertise of chemists and engineers. In this article, we undertake a top-down approach, starting from the analysis of the state-of-the-art in process design to reach the atomic scale design of MOF sorbents for gas separations.

Marco Taddei - Dr Marco Taddei is an Assistant Professor of General and Inorganic Chemistry in the Department of Chemistry and Industrial Chemistry at the University of Pisa, Italy. He received both his master's degree (2007) and his PhD (2011) from the University of Perugia, Italy, followed by a postdoctoral stint in the same University until 2014. In 2015/2016, he was a postdoctoral researcher at Paul Scherrer Institute, Switzerland, then moved to Swansea University, UK, for a three-year MSCA COFUND Fellowship. His research is focused on the synthesis, structural characterization, and gas adsorption properties of coordination polymers and metal-organic frameworks.

Camille Petit - Dr Camille Petit is a Professor in the Department of Chemical Engineering at Imperial College London, UK where she leads the Multifunctional Materials Laboratory. Prior to this appointment, she was a postdoctoral researcher at Columbia University. She received her PhD in Chemistry in 2011 from the Graduate Center of the City University of New York and her M. Sc in 2007 from Ecole Nationale Superieure de Chimie de Montpellier, France. Her research focuses on elucidating the fundamentals of porous materials formation, structure, and chemistry to exploit them in interfacial applications, i.e. separation of molecules and solar fuel production.

1. INTRODUCTION

Gas separation processes are a vital industrial activity that enables the purification of chemical feedstock, the removal of pollutants and the control of greenhouse gases emissions.[1,2] Yet, these processes are highly energy intensive: it is estimated that they are responsible for 10-15% of the world's annual energy consumption.[3] This high energy input is due to the predominance of separation methods that involve large amounts of heat to be provided to or withdrawn from the separation unit during the process, such as cryogenic distillation and liquid absorption. Alternative technologies based on either solid adsorbents[4,5] or membranes[6] are seen as attractive options to lower the energy demand of the process and the associated costs.

Adsorption-based separations involve the selective interaction between the surface of a solid adsorbent and one (or more) species in the target gas stream.[4] Depending on the strength of the interaction between the adsorbent and the adsorbate, the phenomenon can be classified as physisorption, if only van der Waals interactions are involved, or as chemisorption, if the formation of coordination/covalent bonds is involved.[7] The strength of the interaction can be quantified by determining the enthalpy (or heat) of adsorption: the more negative (positive) it is, the strongest is the interaction. Since adsorption is typically an exothermic process, the

associated enthalpy of adsorption is negative, whereas the heat of adsorption is given as the inverse of enthalpy (i.e. a positive number) by convention. Here, we will use the term "heat of adsorption". On the other hand, desorption is endothermic, and an energy input is necessary to dissociate the adsorbate from the adsorbent's surface. As such, a chemisorbent will be more prone to bind a certain species than a physisorbent, but it will also require additional energy to be regenerated and used for the next adsorption/desorption cycle. For equilibrium-based separation (see classification in section 2.1), one of the main challenges in developing new adsorbents is in fact hitting a sweet spot, in terms of heat of adsorption, that allows to preferentially bind one species over others present in the target stream, without requiring an excessive energy input for regeneration.[8]

Solid adsorbents are a diverse class of materials, ranging from amorphous to crystalline, from inorganic to organic to inorgano-organic, from micro- to mesoporous.[8–11] The most common types of adsorbents employed in industrial gas separation processes are zeolites and porous carbons, owing to their low cost, availability on a large scale and good performance. Zeolites are microcrystalline and microporous aluminosilicates, some of which naturally occurring, that display high thermal and chemical stability.[12–14] Zeolites feature narrow pore size distribution, which can be tuned by exchanging the extra-framework cations. However, they are limited in terms of possibilities of functionalisation, which is mainly achieved by tuning the Si/Al ratio.[15–17] Furthermore, with just 239 known zeolite frameworks,[18] there is a limited pool of candidates to choose from. Porous carbons are amorphous sorbents that can be easily prepared by pyrolysis of organic matter, including biomass or polymer waste, which aligns well with circular economy objectives.[19,20] Often an activating agent, such as KOH, is added to favour the formation of small micropores, which are desirable for effective gas separation.[21–25] Porous carbons exhibit an amorphous nature, often with a rather large pore size distribution. Their surface chemistry can be modified by the introduction of heteroatoms such O, S, N and P as well as the impregnation of metal-based species.[26–29] The disordered and heterogeneous nature of porous carbons can make it difficult to predict the best structure and chemistry needed for a given separation.

Metal-organic frameworks (MOFs) are a subclass of coordination polymers, most often characterised by high crystallinity and large porosity, built from the connection of metal cations (or clusters thereof) and organic linkers (carboxylates, azolates, N-heterocycles, phosphonates, sulfonates).[30–34] Details about each MOF mentioned herein, such as the meaning of each acronym used to name MOFs, the structural formulas of organic linkers, the metal ion, and the MOFs chemical formulas, are collected in the Electronic Supplementary Information. MOFs have progressively gained a privileged spot among adsorbents in academic research, thanks to the ease in fine tuning their structure to the atomic level and, in turn, their physicochemical properties, including adsorption properties. The huge chemical space available to build MOF structures – more than 50 metal species plus a virtually infinite pool of organic linkers – makes them stand out, if compared to other adsorbents that offer much less freedom in terms of chemical functionalisation and structural control. Furthermore, being predominantly crystalline materials, MOFs often display narrow and well-defined pore size distributions, mostly in the

microporous regime, which is desirable for separation purposes. Ever since the inception of the field, MOFs have been seen as very promising candidates in the field of gas separation and storage.[35–40]

Until recently, most studies on MOFs for gas separations have focused on the methods to tune the framework structure and pore chemistry to improve the affinity of the sorbent for a certain species of interest.[38,41,42] However, these endeavours have mainly rested in the hands of chemists and have rarely offered a view beyond materials design and development, which becomes detached from the stage of process integration. In recent years, there has been, however, an increasing number of studies focusing on large scale process simulation, which aim to screen existing MOFs to identify the most promising ones, based on engineering-centred criteria.[43–55] In addition, recent reports have adopted an inverse engineering approach and have started to highlight desirable material features - albeit at a rather high level - that are driven by process modelling.[48,50,56–58] A successful adsorption-based gas separation application depends on the identification of the most appropriate sorbent/process combination, which demands that the engineer and the chemist have an understanding of each other's work. On the one hand, the engineer should be aware of how the sorbent is made and how it functions to be able to design a process that can valorise its strengths and circumvent its weaknesses. On the other hand, the chemist or material scientist should know what the process requirements are, to engineer the sorbent at the atomic level and maximise its performance. Hence, a synergy must be established between the two parties, to accelerate the development of efficient adsorption-based gas separation processes.

The scope of this review is to provide chemists, materials scientists and engineers with an overview of the state of the art and of the main challenges in the field of adsorption-based gas separations using MOFs. In doing this, we undertake a top-down approach, starting from the analysis of the state of the art in process design to reach the atomic scale design of MOF sorbents for gas separations. The paper is centred on MOFs, though parts of the discussion also apply to other sorbents. It reports on the current state of adsorbent and adsorption process development and provides the authors' perspectives on the on-going challenges in the field and areas to expand/explore in the future. It does not aim to be a full account of all the studies reported on the synthesis and use of MOF for adsorption-based gas separations but rather to highlight specific trends in the field.

2. OVERVIEW OF GAS SEPARATION PROCESSES

An ideal adsorption-based gas separation process can be represented as in Figure 1. For the sake of simplicity, we here assume the simplest case of a binary mixture, which is a reasonable approximation for many gas separations (see section 2.2 and Table 1). The feed is forced through - typically - a fixed bed of sorbent in compacted or structured form (pellets, beads, extrudates, monoliths), where one species is preferentially adsorbed (heavy product or extract).

The second species (light product or raffinate) breaks through after a short time. The effluent is therefore enriched in light product. The bed becomes progressively saturated with the heavy product and the adsorption step is ended before the heavy product breaks through. Regeneration of the bed can be accomplished via either temperature swing adsorption (TSA), i.e. by increasing the temperature of the bed to a value above that of the feed, or pressure swing adsorption (PSA), i.e. by reducing the pressure to a value below that of the feed. When the pressure of the feed is atmospheric, a regeneration process involving decrease of pressure is termed vacuum swing adsorption (VSA). In both cases, the aim is to put the sorbent in a condition where its uptake capacity for the heavy product is lower than in the adsorption step, thus inducing desorption. One of the main differences between TSA and PSA/VSA is the form in which energy is delivered to the system. In TSA, a source of heat is needed, either waste heat or steam, ideally originated from another process in the proximity of the gas separation rig. PSA/VSA require instead only electricity to operate the pumps needed to compress/evacuate the system. The amount of heavy product recovered during the regeneration step defines the working capacity of the sorbent. Regardless of whether the target product is the light or the heavy one, working capacity must be maximised. In some instances, it could be advantageous to combine temperature and pressure/vacuum swing to achieve better regeneration and, hence, higher working capacity. Once the bed is regenerated, a new cycle is started. Most often, at least two beds are employed to ensure continuity of operation: while one bed is in the adsorption step, the second is undergoing regeneration. The product of interest can be either the light or the heavy one, or both. Often, recovering the light product is preferred, due to a simplified process implementation, especially in terms of attaining high purity.

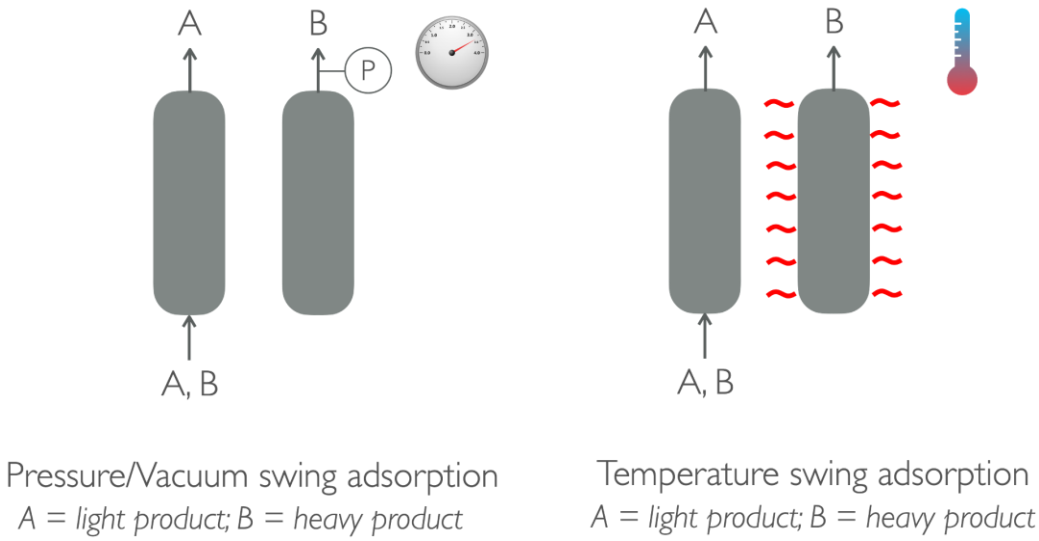

Figure 1. Simplified schematic of a pressure/vacuum swing adsorption process (left) and a temperature swing adsorption process (right).

2.1 Separation mechanisms

At the microscopic level, the separation process can occur via three main mechanisms: equilibrium (thermodynamic), kinetic and molecular sieving (Figure 2).[38,39,59] Regardless of the underlying separation mechanism, the preferentially adsorbed species becomes the heavy product in the ideal separation process seen in the previous section. Equilibrium separations exploit the different binding affinities of the sorbent for the species composing the feed. There are no significant barriers limiting diffusion of the adsorptives through the framework, so that adsorption equilibrium is reached simultaneously. Selectivity mainly results from different heats of adsorption: the adsorbate displaying the higher heat of adsorption is preferentially adsorbed. Surface chemistry is crucial to control the interaction between the sorbent and the adsorbate. Kinetic separations result from significant differences in diffusional behaviour between the two adsorptives. The species that diffuses faster is selectively adsorbed, regardless of whether it displays the highest heat of adsorption. Therefore, kinetic separation can even occur with inverse selectivity from what would be expected based on thermodynamic considerations alone. Prolonged exposure to the feed can lead to decrease in selectivity, as adsorption of the slowly diffusing fraction progressively reaches equilibrium. Kinetic separation is usually achieved by tuning the pore size of the sorbent to a value approaching the kinetic diameter of the largest molecule, thus hindering its diffusion to a larger extent than that of the smaller one. Kinetic separation is often mentioned in tandem with membrane technology, but it can be accomplished in fixed beds as well, although it is not widely employed in industrial settings yet.[22] Sieving separations are an extreme version of kinetic separations, where one of the species is completely prevented from diffusing within the framework and breaks through instantaneously. Again, control of the sorbent's pore size becomes crucial, as in this case the pore limiting diameter must fall in between the kinetic diameters of the two molecules. Infinite selectivity is achieved with molecular sieving, as one of the species is never adsorbed.

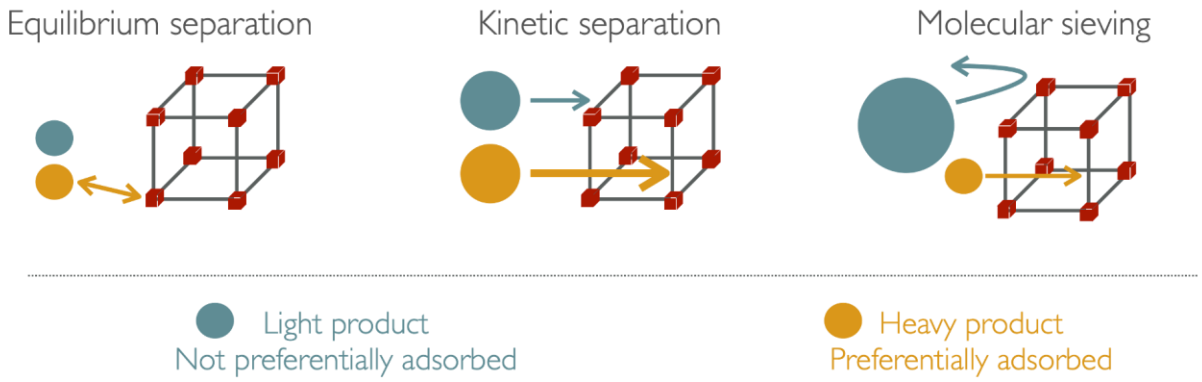

Figure 2. Schematic overview of the various adsorption-based separation mechanisms.

2.2 Gas separation processes of significant interest

Table 1 provides an overview of gas separations of significant interest, which are briefly described herein. We focus here on examples of adsorption-based separations and strictly consider the separation of gaseous species and not vapours or liquids. As a result, we have for instance not included water harvesting using MOFs and interested readers are directed towards other reports.[60–64]

Table 1. Details of important gas separations where adsorption plays/can play a role.

Separation	Feed composition	Main impurities	Feed conditions	Process	Minimum Requirements
Postcombustion CO_2 capture	N_2/CO_2 4-25% CO_2	H_2O, CO (steel), SO_x, NO_x, H_2S	1 bar, 40-90 °C	TSA, VSA, VTSA	90% recovery, 95% purity (CO_2)
Direct air capture	$N_2/O_2/CO_2$ 0.04% CO_2	H_2O, Ar	1 bar, RT	TSA, VTSA	95% purity (CO_2)
Precombustion CO_2 capture	H_2/CO_2 15-25% CO_2	CH_4, CO, N_2	8-28 bar, 21-38 °C	PSA	90% recovery, 95% purity (CO_2) 70-90% recovery, 99.999%purity (H_2)
Biogas upgrading	CH_4/CO_2 30-55% CO_2	N_2, H_2O, H_2S	1-5 bar, RT	PSA, VSA, PVSA	90% recovery, 95% purity (CO_2) 98% purity (CH_4)
Natural gas sweetening	CH_4/CO_2 0-43% CO_2	H_2S, H_2O	20-70 bar, RT	PSA	90% recovery, 98% purity (CH_4)
Air separation	N_2/O_2 20% O_2	H_2O, Ar	1-10 bar, RT	PVSA	95% purity (O_2)
Acetylene purification	C_2H_2/CO_2 3.5% CO_2	H_2, CO, CH_4	1 bar, RT	PVSA	98% purity (C_2H_2)
Acetylene/ ethylene	C_2H_2/C_2H_4 1% C_2H_2	-	1 bar, RT	PVSA	99.9% purity (C_2H_4) < 2 ppm (C_2H_2)
Ethylene/ ethane	C_2H_4/C_2H_6 50% C_2H_6	-	1 bar, RT	PVSA	99.5% purity (C_2H_4)
Propylene/ propane	C_3H_6/C_3H_8 50% C_3H_8	-	1 bar, RT	PVSA	99.5% purity (C_3H_6)

2.2.1 Postcombustion carbon capture

Postcombustion carbon capture[65–67] can be applied to a variety of large point sources (i.e. coal-fired power plants, gas-fired power plants, steel, cement, petrochemical industry) and can be approximated to a CO_2/N_2 separation, with CO_2 as the heavy product and N_2 as the light product. Separation of CO_2 from N_2 can be accomplished both via thermodynamics - taking

advantage of the large quadrupole moment of CO_2 (4.3×10^{-26} esu cm^{-2}) that makes it more prone than N_2 (1.4×10^{-26} esu cm^{-2}) to interact with polar surfaces - and kinetics, by exploiting the difference in kinetic diameter between CO_2 (3.3 Å) and N_2 (3.6 Å).[68,69] The former tends to be most studied. Depending on the source, the concentration of CO_2 can vary between 4% (gas fired power plants) and 25% (blast furnace gas). Major impurities include H_2O (5%), CO (20-25% in blast furnace gas) and acid gases, such as SO_x, NO_x and H_2S, in lower amounts. The feed is at atmospheric pressure and a temperature in the range 40-90 °C. Regeneration can be accomplished either via TSA, VSA or VTSA. The target CO_2 recovery and purity, as indicated by the US Department of Energy, are 90% and 95%, respectively. Since the effluent (mainly N_2) is vented into the atmosphere, there is no requirements recovery and purity of the light product. The state-of-the-art technology for this separation is amine scrubbing, based on chemical absorption.[70] Adsorption-based alternatives are becoming increasingly more competitive. Notably, a MOF-based TSA process has recently been implemented by Svante to capture CO_2 from a cement plant in Canada employing CALF-20, based on Zn^{II}, 1,2,4-triazole and oxalic acid.[71–73]

2.2.2 Direct air capture (DAC) of CO_2

DAC[65,66,74,75] has become a highly sought-after technology, thanks to its potential to enable negative CO_2 emissions, if coupled with permanent geological storage. Even though the composition of air is about 80% N_2, 20% O_2, 0.04% CO_2, DAC can be approximated to a CO_2/N_2 separation, because of the similar adsorption behaviour displayed by N_2 and O_2 in most cases, owing to their similar physical properties (i.e. kinetic diameter, quadrupolar moment, polarizability). As in the case of postcombustion capture, CO_2 is the heavy product and N_2 the light product. The feed is at ambient conditions, both in terms of pressure and temperature, and its relative humidity varies depending on geographical location, season, and time of the day. The concentration of CO_2 is 415 ppm (0.04%), about two orders of magnitude lower than that present in the exhaust of a gas-fired power plant. Adsorption of such ultra-dilute CO_2 is associated with a large loss of entropy, making a high heat of adsorption necessary to render the process spontaneous. For this reason, TSA is the preferred regeneration method, but a mild vacuum can also be applied to improve the working capacity of the sorbent. Different from postcombustion and precombustion capture, in this case there is no set target recovery as yet, as the feed and the raffinate are basically the same thing, minus some ppm of CO_2. The captured CO_2 must still be more than 95% pure for downstream processing. Chemical adsorption using amine-based sorbents is already one of the state-of-the-art technologies for this separation, along with chemical absorption employing alkali solutions.[76]

2.2.3 Precombustion carbon capture

Precombustion carbon capture[65–67] involves generation of a CO/H_2 mixture (syngas) by either steam methane reforming, coal gasification or biomass gasification, which is subsequently converted to a CO_2/H_2 mixture via the water-gas shift reaction.[77] Removal of CO_2 from the mixture allows to combust pure H_2, yielding only water as a by-product. Precombustion capture

can be approximated to a CO_2/H_2 separation, with CO_2 as the heavy product and H_2 as the light product. The separation is primarily driven by thermodynamics, because of the typically much weaker interaction of adsorbents with H_2 than with CO_2. The feed composition primarily depends on the feedstock used for generating the syngas and the concentration of CO_2 in the feed can vary between 15 and 25%. The feed is usually at a pressure comprised in the 8-28 bar range and temperature between 21 and 38 °C.[78] Major impurities include CO, CH_4 and N_2. Precombustion capture is typically performed in PSA conditions, taking advantage of the high pressure of the feed for the adsorption step. The same concept can be extended to the purification of H_2 for either use as a reductant to produce chemicals, such as ammonia, and steel, or in fuel cells. As for post combustion capture, the target CO_2 recovery and purity are 90% and 95%, respectively. However, in the case where H_2 is to be used as a reagent or in a fuel cell, there is also a constraint on H_2 recovery (70-90%) and purity (98–99.999%). The state-of-the-art technology for this separation is based on physical absorption, employing a glycol-based solvent, but the relatively high partial pressure of CO_2 in the feed makes adsorbents an attractive alternative.

2.2.4 Biogas upgrading

Recovery of CH_4 from biogas (biogas upgrading)[79] has a two-fold purpose: it prevents venting of CH_4, a highly potent greenhouse gas, in the atmosphere from sources such as landfills and biomass fermenters, and it provides a fuel with high energy content and a well-developed infrastructure for transport. Biogas upgrading can be approximated to a CH_4/CO_2 separation, with CO_2 as the heavy product and CH_4 as the light product. The percentage of CH_4 in the feed can range between 45-70%, depending on the source.[80,24,81] The separation mechanism can be either thermodynamic, driven by the quadrupole moment of CO_2 (CH_4 has no quadrupole moment), or kinetic, because of the smaller kinetic diameter of CO_2 (3.3 Å vs 3.8 Å for CH_4).[68] The feed is available at atmospheric pressure and room temperature, but it can be compressed to pressures up to 5 bar, if this leads to improvements in recovery and purity. Regeneration can be accomplished via either PSA, VSA or PVSA. Main impurities include water (saturated feed), N_2 (0-3 %), H_2S (< 1%) and NH_3 (0.01%). The CH_4 produced must be of pipeline quality, i.e. with purity higher than 98%, due to potential issues with pipe corrosion. In terms of recovery, there are no specific guidelines, but values exceeding 95% can be achieved with different technologies. At present, there is no single technology that can be considered state-of-the-art for biogas upgrading, as chemical absorption, physical absorption, membrane separation and adsorption are all deployed industrially.[24,82]

2.2.5 Natural gas sweetening

Akin to biogas upgrading, sweetening of natural gas can be approximated to a CH_4/CO_2 separation, with CO_2 as the heavy product and CH_4 as the light product.[83,84] Removing acid gases (CO_2 and trace H_2S) is necessary to prevent pipeline corrosion and, in case of natural gas liquefaction, formation of solid CO_2. The amount of CO_2 to remove highly depends on the well and can reach up to 42%. The feed's pressure can range between 20 and 70 bar, while the

temperature is ambient, making PSA the preferred process. The stream can contain water as the main impurity, sometimes at saturation levels, whereas the amount of H_2S can be as high as 3%. In terms of recovery and purity, the same constraints mentioned above for biogas upgrading are applied. As in the case of biogas upgrading, different technologies are in use for natural gas sweetening.

2.2.6 Air separation

Air separation is primarily carried out to produce pure O_2 for medical purposes or for usage in the steel industry (basic oxygen steelmaking), but recovery of pure N_2 is also of interest as a feedstock for ammonia production, inert gas or as a cryogenic liquid.[85,86] Air separation is also necessary for oxyfuel combustion, which involves combustion of a fuel in pure O_2, producing a high purity CO_2 stream that only requires condensation of water before downstream processing.[65,66] It is basically an O_2/N_2 separation, primarily driven by thermodynamics, in which N_2 (78% concentration in the feed) or O_2 (20% concentration in the feed) can be either the light or the heavy product. This depends on what is the purified species of primary interest, which is preferentially recovered as the light product. Air separation is usually performed in PVSA conditions, compressing the feed at RT up to 10 bar in adsorption and applying vacuum to regenerate the sorbent. The strictest requirement is purity, which must be at least 95% for O_2 and N_2 alike, whereas recovery is not constrained, although its maximisation is desirable for economic reasons. Air separation on a large scale is performed by cryogenic distillation, but portable O_2 concentrators for medical purposes are based on a PSA system that employs zeolite LiX as the adsorbent.[85–87]

2.2.7 Acetylene purification

Acetylene (C_2H_2) is an important fuel and chemical feedstock, which is commonly produced by partial combustion of natural gas.[88–91] This process produces a rather complex gas stream, where C_2H_2 (7-9%) is diluted in significant amounts of H_2 (42-56%), CO (26-38%), CH_4 (5%) and CO_2 (3.5%). The feed can be pressurised, provided that the partial pressure of C_2H_2 is kept below 1.4 bar, due to danger of explosion. The most challenging task is to separate C_2H_2 from CO_2, because the two species have similar physicochemical properties (quadrupole moment is 4.3×10^{-26} esu cm^{-2} for CO_2 vs 3.0×10^{-26} esu cm^{-2} for C_2H_2) and nearly identical size (kinetic diameter is 3.3 Å for both molecules).[37] Therefore, most literature reports dealing with adsorption based C_2H_2 purification focus on the binary C_2H_2/CO_2 separation. Adsorption of C_2H_2 is often thermodynamically favoured over CO_2 in physisorbents, therefore C_2H_2 has to be recovered during the regeneration step. Sorbents with reversed C_2H_2/CO_2 selectivity are desirable to enable easier recovery of C_2H_2. Kinetic separations are not reported for this mixture. The main requirement is acetylene purity, which must be at least 98% for use in oxyacetylene welding and 99.7% for most applications as a chemical feedstock.[39] Currently, C_2H_2 is extracted from gas mixtures by absorption using organic solvents (e.g. *N*-Methylpyrrolidone, *N*,*N*-Dimethylformamide), generating a large amount of hazardous solvent waste.[88]

2.2.8 Acetylene/ethylene separation

Another important separation involving acetylene is the removal of trace amounts (< 1%) of this gas from ethylene (C_2H_4) produced by steam cracking. Since even trace amount of alkyne can poison the catalyst during polymerisation of C_2H_4, the concentration of C_2H_2 must be kept below 2 ppm.[37,39,88,92] Acetylene is usually preferentially adsorbed over ethylene, owing to its higher quadrupole moment (3.0×10^{-26} esu cm^{-2} vs 1.5×10^{-26} esu cm^{-2} for ethylene) and increased acidity of H atoms, which can lead to favourable hydrogen bonding interactions with the sorbent.[37] In addition, acetylene has much smaller kinetic diameter than ethylene (3.3 Å and 4.16 Å, respectively), making kinetic separation possible. Thus, acetylene is usually the heavy product, the ideal situation to recover purified ethylene as the light product during the adsorption step. The current industrial process to remove acetylene impurities from ethylene is cryogenic distillation. Other technologies, including adsorption, are not yet mature enough to be considered for the scope.[88,92]

2.2.9 Olefin/paraffin separation

Besides the alkyne component, the uncracked paraffin fraction, i.e. ethane (C_2H_6), must be removed from the ethylene stream to achieve the high purity needed for the polymerisation process.[39,92] The same applies to propene (C_3H_6), another critical chemical feedstock for polymer production, which contains uncracked propane (C_3H_8) as a major impurity.[93] In both cases, 50:50 olefin/paraffin binary mixtures are assumed, and the goal is to obtain polymer grade olefin (purity > 99.5%). Olefin adsorption is usually thermodynamically favoured, owing to the electron density of the double bond that makes them more amenable to engage in van der Waals interactions with the sorbent. The small size difference between ethylene and ethane (kinetic diameter of 4.16 Å and 4.44 Å, respectively) makes kinetic separation challenging, although a few examples have been reported.[94,95] The situation is even more challenging in the case of propylene and propane (kinetic diameter of 4.5 Å and 4.3 Å, respectively) and examples of kinetic separations are scarce in the literature.[96,97] In all instances, the olefin is the heavy product and has to be recovered once the adsorption step is finished. For this reason, sorbents displaying inverse selectivity would be preferred, even though it has been rarely observed.[98] Since the paraffin is also the least abundant component of the feed, inverse selectivity would also allow the usage of smaller beds, with considerable savings.[37] The state-of-the-art process for olefin/paraffin separation is distillation, which is conducted at high pressure (20 bar) with a large number of trays, due to the similar boiling points of the species involved.[99] This process is highly expensive, but at present valid alternatives have not yet been identified.

3. Overview of process and sorbent parameters

The above section explored the specificity of different gas separation challenges. Here, we instead take a broader look at some 'universal' links between the adsorbent properties and the separation process performance. These links can influence how we approach and address a separation challenge. To help our discussion, we introduce four categories that broadly cover gas separation aspects from the atomic scale to the process scale. Figure 3 presents such categories with specific examples and Table 2 describes some of the metrics and properties. The four categories include: sorbent inherent properties, sorbent emergent properties, material sorption metrics and process metrics. We term sorbent inherent properties the features of a MOF that can be designed and engineered at the atomic level by using the principles of reticular chemistry (e.g. surface area, surface chemistry). With sorbent emergent properties, instead, we identify properties, such as heat capacity and thermal conductivity, that have been less intensely investigated in MOFs, but bear a significant influence in a separation process. Material sorption metrics correspond to measures derived from the isotherms and breakthrough profiles of a sorbent (e.g. working capacity, selectivity). Finally, process metrics refer to measures of the industrial/deployment potential of a sorbent for given process conditions (e.g. sorption cycle, temperature, pressure). We note that this section of the article is rather 'agnostic' to the type of adsorbent utilised and extends to all types of adsorbents, MOFs and beyond. Having introduced this classification, we now highlight selected links between elements of each category.

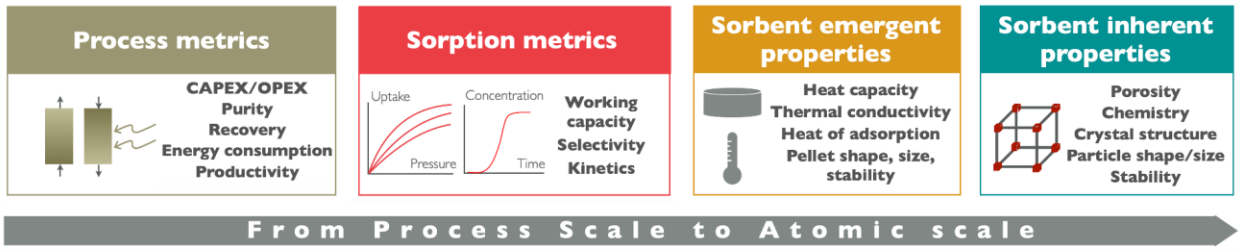

Figure 3. Classification of process and materials metrics and properties used to describe and assess sorbents for a given separation.

Table 2. Summary of some of the process and sorption metrics as well as sorbent emergent properties used to assess and characterise sorbents.

Metric	**Definition/Notes**	**Units**
CAPEX	Total capital expenditure	\$
OPEX	Annual operating costs	$\$\ year^{-1}$
Energy consumption	$\frac{\sum_{i=cycle\ configuration} E_i}{Adsorbate\ of\ interest\ mass\ in\ the\ extract\ product\ per\ cycle}$	$\frac{kWh_e}{tonne\ adsorbate\ in\ extract\ product}$
Purity	$\frac{Total\ moles\ of\ adsorbate\ of\ interest\ in\ the\ extract\ product}{Total\ moles\ of\ species\ in\ extract\ product} \times 100$	%
Recovery	$\frac{Total\ moles\ of\ adsorbate\ of\ interest\ in\ the\ extract\ product}{Total\ moles\ of\ species\ in\ feed} \times 100$	%
Productivity	$\frac{Total\ moles\ of\ adsorbate\ of\ interest\ in\ the\ extract\ product\ over\ 1\ cycle}{(Total\ volume\ of\ adsorbent)\times(Cycle\ time)}$	$mol_{adsorbate}\ m^{-3}_{adsorbent} s^{-1}$
Working capacity	$Gas\ uptake\ under\ adsorption\ conditions - Gas\ uptake\ under\ desorption\ conditions$	$mol\ kg^{-1}$
Heat capacity	Amount of heat required to produce a unit change of temperature in the sorbent.	Molar: $J\ mol^{-1}\ K^{-1}$ Specific: $J\ g^{-1}\ K^{-1}$
Thermal conductivity	The ability of the sorbent to conduct heat.	$J\ m^{-1}\ K^{-1}\ s^{-1}$
Heat of adsorption	Amount of heat evolved during the adsorption step. It relates to the strength of adsorption of a given adsorbate on a given sorbent.	$J\ mol^{-1}$

3.1. Links between process metrics

We start with examples of links between process metrics themselves. Expectedly, OPEX and energy consumption are directly connected as by definition, OPEX encompasses any operational cost, including any energetic requirements to drive the process, particularly the desorption step. These energy requirements include for instance applying vacuum in the case of a VSA process or heating the column in the case of a TSA process. Overall, utilities often make up for a large portion of the OPEX.[100] We can also cite a link between CAPEX and productivity: CAPEX decreases with an increase in productivity. Productivity is defined as the amount of product per unit of volume of the sorbent, per unit of time. Hence, if the productivity increases, less sorbent and possibly a smaller bed are required, thereby decreasing CAPEX.

3.2. Links between process metrics and material sorption metrics

We now turn our attention to examples of links between process metrics and material sorption metrics, such as purity and selectivity. As selectivity increases, more of the product of interest is adsorbed (assuming the heavy product is the product of interest). As a result, during regeneration/desorption, less of the light product will be present in the gas stream, thereby enhancing the product purity. The importance of selectivity for the sake of purity, particularly in comparison to other material sorption metrics such as working capacity, has been highlighted in many reports on CO_2 capture in the recent literature.[48,50,101] We can also discuss the link between working capacity and recovery. Recovery is defined as the ratio between the amount of product generated over the amount of product in the feed stream. If the working capacity increases, more of the product is recovered. It is important to note here that working capacity is different from adsorption capacity. Working capacity takes into account the regeneration of the material, which is critical for recovery. In other words, a sorbent can exhibit a high sorption capacity but a low recovery if it still adsorbs a lot of product at the desorption conditions.[50,101] We also observe the link between CAPEX and working capacity. In the case of VSA, the working capacity of a sorbent may imply the use of a certain vacuum level which in turn will drive the choice of the vacuum pump. The vacuum pump is part of the CAPEX. Similarly, the working capacity will influence the vessel size – a low working capacity requires more adsorbent and therefore a larger vessel – which is also part of the CAPEX. Working capacity also influences OPEX. Along the same line, as discussed above for the link between working capacity and CAPEX, the working capacity of a sorbent will drive the use of a certain vacuum level to be applied during a VSA operation. Finally, one can connect productivity and sorption kinetics. The quicker the adsorption and desorption steps take place, the shorter the cycle time and therefore the higher the productivity.

3.3. Links between process metrics and sorbent emergent properties

Now that we understand how some material sorption metrics influence process metrics, it is important to look at how a material can influence a process and vice versa. For this, we consider links between sorbent emergent properties and process metrics. We look first at CAPEX and heat of adsorption. In an adiabatic scenario, a high heat of adsorption leads to a large temperature swing during the adsorption step due to the exothermic nature of adsorption. This large temperature swing in turn reduces the amount of adsorbed molecules and therefore reduces the working capacity. The reduced working capacity decreases productivity and therefore the CAPEX, as explained in section 3.2. We also highlight the link between CAPEX and heat capacity. A high heat capacity limits the temperature swing during sorption. Therefore, in a TSA process, for the same energy input used to drive desorption, the working capacity increases, which helps the CAPEX. OPEX and heat capacity are also linked. In a TSA process, the heat capacity increases the energy requirement (i.e. OPEX) to achieve the same temperature swing. On the contrary, for a PSA process, a high heat capacity is preferred as it buffers temperature swings upon adsorption and desorption, thereby maintaining the working capacity and therefore OPEX. In a study by Huck et al.[102] on adsorbent evaluation for CO_2 capture, the link between enthalpy, heat capacity and parasitic energy, which relates to OPEX, is investigated. In a TSA process, a low heat capacity also makes it easier/faster to cool down the bed, which can help productivity. Finally, the pellet size, morphology and porosity will influence the process performance. As pellet porosity increases, the amount of adsorbent packed decreases, and so do the working capacity and productivity. This relates to the importance of volumetric capacity. Yet, an increased porosity also enhances mass transfer which positively impacts productivity. The pellet porosity also relates to the recovery. As the pellet porosity increases, more gas is present in the pellet macropores (i.e. interparticle pores, extrinsic to the sorbent), especially the light product (i.e. product not of interest). This effect leads to a decrease in purity. As the pellet size decreases, the pressure drop across the vessel increases, which enhances the energy demand. The multifaceted impact of manufacturing of the sorbent pellets are described in depth in a recent paper by Farmahini et al.[47]

3.4. Links between material sorption metrics and sorbent inherent properties

Focusing more on material science and chemistry, we now look at how selected sorbent inherent properties control material sorption metrics. Surface area will lead to an increased uptake, irrespective of the adsorbate. This reduction in adsorbates discrimination directly impacts the selectivity. This is a situation to avoid when the light product is not the desired one as in the case of CO_2/N_2 separation.[48,50,101] In addition, the crystal density and porosity will influence the micropore diffusion, which can play a role in the overall kinetics of the sorption process.

3.5. Links between sorbent emergent properties and sorbent inherent properties

Naturally, sorbent inherent properties directly influence the sorbent emergent properties. An interesting aspect to look at is the link between the nature of the adsorbent and its thermal properties, namely heat capacity and thermal conductivity. The latter is particularly relevant for TSA, for which regeneration requires that heat be diffused homogeneously and quickly throughout the bed. Overall, little knowledge is available in the literature to link thermal properties and sorbent inherent features. Looking specifically at the studies on MOFs, limited data are available on their thermal conductivity and heat capacity.[103–106] Empirical models have been proposed to link the heat capacity of MOFs and their composition.[104] Molecular simulations have also been reported to counterbalance the lack of experimental data and provide fundamental insights in the thermal conductivities,[107–112] as well as heat capacity and thermal expansion of MOFs.[113] These studies explain how both the chemical composition (e.g. functional groups), and the structural features influence the thermal properties. For instance, dense MOFs usually display higher thermal conductivity, but lower specific heat capacity, than highly porous ones.[113] One should also keep in mind that any adsorbed species on the surface of the material will influence the thermal properties. Therefore, a careful desorption must be conducted to experimentally measure the intrinsic thermal properties of the sorbent. Likewise, during an actual sorption process, the thermal properties will evolve as species adsorb on the surface of the material. Here again, theoretical work has mainly been reported to account for the presence of adsorbed species,[114–116] although experimental evidence has also appeared recently.[117] Another important inherent property is the particle size. It will influence the pelletisation process, which ultimately has an impact on the pressure drop. In addition, large crystallites are undesirable because surface barriers start becoming relevant as the size increases, with negative effects on adsorption kinetics and, in turn, on adsorption performance.

3.6. Links between process metrics and sorbent inherent properties

Finally, we look briefly at how sorbent inherent properties can influence process metrics. First, we take the example of sorbent composition and cost. This connection becomes particularly evident when considering MOFs for which the cost will, in part, depend on the cost of the metal as well as that of the linker (sometimes purposely synthesised). The metal and the linker may themselves dictate the type of solvents and/or manufacturing process, which also incur a cost. A study by DeSantis et al.[118] has looked at some of the cost drivers for MOFs synthesis, showing that the solvent and linker play an important role. The authors suggested that choosing a water-based or a solvent-free synthetic protocol could significantly reduce the MOF production cost while enhancing the sustainability of the process.[119] The nature of the MOF also dictates to some extent its mechanical, chemical and thermal stability (see also section 6.1). These aspects in turn influence the number of cycles and the type of conditions (temperature, pressure), the material can withstand during a separation process, which all link to CAPEX and OPEX. This issue, which is one that the MOF community needs to pay attention to, is further complicated by the fact that

the synthesis method and any post-processing steps (and not just the MOF inherent composition) can influence the stability of the MOF.

3.7. General remarks

The above discussion highlights the importance of knowing the links between the different sorbent and process categories to make informed decisions when it comes to addressing a particular separation challenge. This discussion also shows that some links can be in tension. For instance, an increase in working capacity will increase the recovery but possibly the CAPEX too. Similarly, a high pellet porosity will benefit gas diffusion while also decreasing the bed density. As explained above, heat capacity has an opposite impact whether a PSA or a TSA process is considered. Ideally, one would have at their disposal an optimisation framework that captures all these links and tensions. Today, such a framework does not exist, but optimisation work can still be performed on some aspects of the separation as described in the next section. In any case, we can see that trade-offs are unavoidable when addressing a separation challenge. In fact, typical process modelling studies display so-called pareto plots that show the theoretical limit in terms of combined process metrics for a given material. Recently, Pai et al. reported a study that looks at a separation challenge from a different angle and aims to answer the question: "If we can design the ideal adsorbent(s), what are the practically achievable limits of minimum energy and maximum productivity for a PVSA process?"[120] The study focuses on CO_2 capture and shows that even with the best material, a PVSA process might not be competitive from an energy and productivity standpoint, with an absorption process for CO_2 feed stream composed of 15% CO_2 and below.

4. Process simulation studies

Having introduced the links between process and adsorbent in the previous section, we now highlight how studies have exploited these links to answer the following question: "What is the best {sorbent + process} system needed to address a specific separation challenge?". Here, 'best' refers to a system that allows the targets of the given separation (i.e. purity and recovery) to be met at a competitive energy consumption and cost in absolute or with respect to existing or alternative separation technologies. It is important to note that this question implies that the sorbent and the process cycle and conditions are selected in combination. In other words, a process might be well-suited for a given sorbent but not another and *vice versa*.

4.1. Overview of proposed approaches

One way to answer this question is to perform a screening study, the overall approach of which is described in Figure 4 and below.[56,121,122,51,54,55] Screening studies aim to identify the best

process conditions for an adsorbent and to derive a ranking of {sorbent + process} systems for a given separation, considering one or more process cycles. These studies can rely on databases of existing or hypothetical sorbents whose sorption isotherms can be simulated (e.g. using RASPA[123]). For crystalline sorbents, such databases exist and one can cite the Cambridge Structural Database (CSD) MOF subset,[124,125] the CoRE MOF database,[126,127] or the Zeolite Structures Database.[18] The use of these databases makes it relatively straightforward to eliminate certain structures based on simple metrics, e.g. nature of the metal (e.g. toxic metal), pore size (e.g. too small for adsorption), etc. When databases cannot be used (e.g. for non-crystalline sorbents), one can use experimental isotherms data reported in the literature. Indeed, for these cases, it might not be possible/easy to model sorption isotherms. The subsequent step is to determine an analytical expression of the isotherms, which can be obtained by fitting the isotherms with known models (e.g. single-site or dual-site Langmuir models among others). The isotherms of all species involved in the separation must be known/calculated. Without this, a process evaluation is impossible. This aspect is particularly important to remember when carrying out experimental studies for which there tends to be a focus on the adsorbate of interest. Equally important is to collect isotherms at, at least, three temperatures to allow a calculation of the heat of adsorption, which is a parameter included in the process evaluation. Once the isotherms have been expressed analytically, the screening can be done using either detailed or simple process models. Optimisation can then be applied to target a specific objective function, e.g. 'minimise energy'. This way, the screening allows to achieve an optimal energy consumption for a set target of purity and recovery. In this optimisation step, the process conditions typically become variables to optimise. Such screening/optimisation approach can be done for a given cycle or for different cycle configurations, thereby allowing a comparison between different cycles.[54,128,129] Once a manageable – from an experimental viewpoint – number of sorbents have been identified, detailed experiments can be performed to fill in knowledge gaps required for further development and to validate some of the assumptions of the process models.

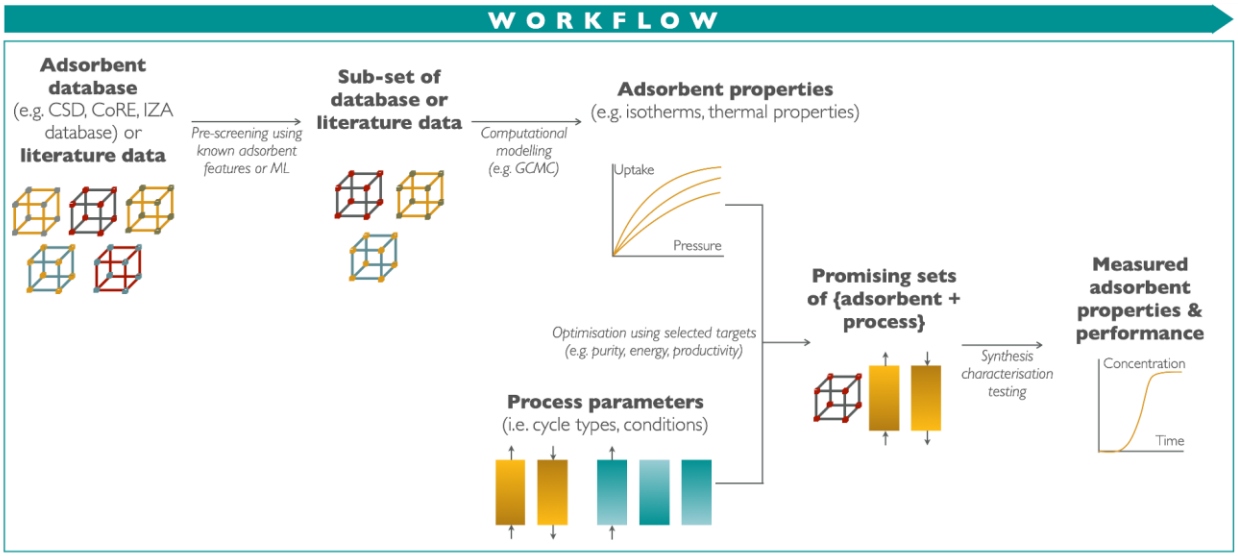

For simplicity, feedback loop/validation steps are not shown but exists between the steps described here

Figure 4. Schematic describing steps of the sorbent screening approach using process modelling.

In addition to screening, process modelling can be used as a reverse engineering approach. Here, the aim is to identify the features of the best adsorbent considering one or more processes. Such an approach does not rely on database or literature data. Instead, the isotherm parameters (or material characteristics driving the isotherms) become the variables of the optimisation process.[57,56,48,58,50] These include for instance Henry's constant, heat of adsorption, or gas uptakes. Based on these measures, material scientists can aim to design an adsorbent that displays the desired features identified by the reverse engineering approach.

In either the screening approach or the reverse engineering approach described above, process modelling can help drive the experimental work and allow it to be focused on the most promising sorbents. In recent years, these approaches have been preferred to the use of 'simple' sorbent metrics that have been proposed earlier. The 'simple' sorbent metrics include the ones we described in the above section (e.g. working capacity, selectivity, regenerability) as well as figures of merits defined to combine two or more sorbent metrics.[130–132,101] It has been shown that such metrics do not allow a reliable ranking of the sorbents, though they often allow to eliminate poor sorbents.[47,51,52,101,121,133] The reason for this is that, as highlighted in the prior section, multiple links – some in opposition – exist between these metrics. The complexity of these links is well conveyed in the studies by Huck et al, which dedicates a section of their study to describing any trend between the process metric of parasitic energy and 'simple' sorbent metrics.[102] While the study shows that a single metric can give useful insights into a material, it is not sufficient to determine the optimal sorbent. Despite the above conclusion, one should recognise that in some cases, sorbent metrics can be used as reasonable proxies of process-level performances. This was shown by Park et al. for a specific sub-ambient PSA cycle for CO_2 capture using MOFs.[133]

4.2. Current challenges

While there is increasing focus on how one can identify a suitable {sorbent + process} system for a given separation, there remains many challenges to be addressed. We review such challenges that the community will have to overcome going forward. They are also visualised in Figure 5.

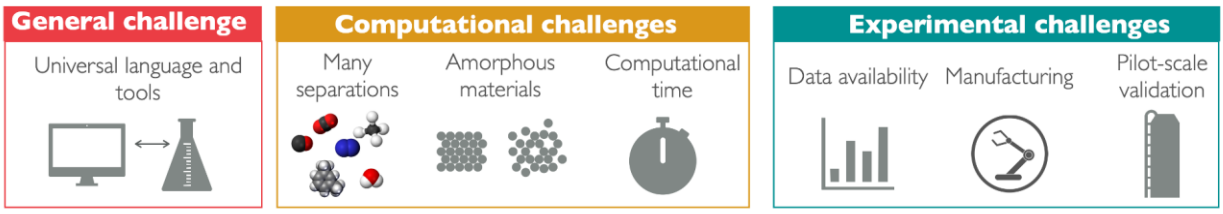

Figure 5. Overview of some of the challenges to overcome when identifying {sorbent + process} system for a given separation.

4.2.1. Extending the approach to various separations

The first challenge to overcome has to do with scope. For now, most of the {sorbent + process} system optimisation work has been reported in the context of CO_2 capture (particularly for high CO_2 inlet concentrations). As described in Table 1 and section 2, several other gas separations exist, and one could envision a similar approach to be implemented. For this to happen, it helps to consider separations for which there are known targets and maybe an existing benchmark technology to compare to. Generating isotherms that can also be used as input/validation data for the process models is also important.

4.2.2. Exploiting data and databases

As described above, the screening approach relies so far on GCMC or experimental data reported with sufficient level of details and at the relevant conditions. What if these data are not available? In the case of amorphous materials (including MOFs), what if GCMC cannot be easily applied? At that point, a repository of adsorption isotherms can become useful. The National Institute of Standards and Technology (NIST) is moving into that direction and has created a searchable database of isotherms (ISODB). Information on the adsorbent, adsorbate and temperature can be used to search isotherms.[134–136] The tool allows visualisation as well as direct extraction of the data points. At this time, the database counts about 32,000 isotherms (300 adsorbates, 6000 adsorbents) and is continuously updated. In the same spirit, Evans et al. have recently proposed the use and deployment of adsorption information files, AIF, similar to crystallographic information files, CIF.[137] This paper presents a universal format for reporting adsorption isotherms following the STAR format.[138] One can imagine that if researchers start reporting isotherms in this format, the updating of sorption isotherms databases will become easier. In fact, AIF like CIF today might become a requirement when publishing. One should keep in mind that the accuracy of the experimental isotherms from databases rely on the quality and conditions of the measurements. In any case, as such experimental isotherm databases grow, the use of machine learning approaches to conduct the screening of adsorbents becomes easier and particularly attractive for amorphous materials. A review of current machine learning studies applied to adsorption recently published in the context of CO_2 capture[139] and covers trends in the current literature.[140–142] Importantly, machine learning approaches can not only be applied at the process level as in the studies discussed above but also to predict isotherms[143] as well as to predict the performance of amorphous sorbents.[144]

4.2.3. Generating enough good quality experimental data

Overall, machine learning approaches rely on the availability of sufficient high-quality data, whether they relate to material characterisation (e.g. structural or chemical analysis) or material testing (e.g. sorption test). The question then becomes as to how one can generate sizeable high-quality data. This would first require an ability to synthesise many sorbents, to then characterise them and test their sorption behaviour. In this context, we observe an increase of activity in the field of automated high-throughput synthesis, characterisation and testing which was recently captured in a review article by Clayson et al.[145] While automated high-throughput synthesis platforms are available commercially, the sorption testing stage still largely relies on purpose-

made units to conduct automated tests.[146] We note that automated high-throughput techniques can not only help synthesise, characterise and test sets of existing promising sorbents identified by process modelling but they can also help with sorbents discovery. The latter aspect is covered in section 6.6.

4.2.4. Speaking the same language

Coming back to computational aspects, process simulation and optimisation remain time-consuming, requiring many core hours. In this context, simple models[57] and machine learning approaches[141] can help reduce that time. Yet, one needs to know the limitations and benefits of each type of approach and select it according to a study objective. Linked to this aspect, it is important to recognise that the process modelling tools being developed, while maybe targeting material scientists, are not necessarily easily usable by this community. Eventually, one could envision a universal software with a user-friendly graphical user interface (GUI) dedicated to one or more separation, which would require adsorbent properties as input and provide adsorbent process performance as output. First steps in that direction can be seen in the MOF Data Explorer reported by Fairen-Jimenez et al.[147]

4.2.5. Validating models

Another challenge related to process modelling is the need to validate the cycle performance using pilot-scale tests. Today, the availability of such pilot-scale testing units remains very limited.[148] Yet, they allow using the outputs of the detailed models in absolute rather than relative to other outputs of the same model, as would be done for simple models. Pilot-scale testing units require more investment than lab-scale testing units and one needs to identify the best source to cover work at such TRL.

4.2.6. Investigating poorly understood sorbent properties

Maybe easier to address is the lack of data related to some of the sorbent properties. In particular: sorption kinetics, thermal properties as well as manufacturing and post processing. The accuracy of process simulation can be improved if these properties are known. Therefore, collecting more experimental data and developing computational methods to better describe and predict these properties become key. Looking at sorption kinetics, unlike volumetric and gravimetric sorption instruments, there is no commercial unit that allows direct measurement of sorption kinetics. Instead, one has to rely on other tools to study macropore and/or micropore diffusion, such as zero length column (ZLC),[149] frequency response measurement (FRM), pulse-field gradient (PFG) NMR,[150] interference microscopy (IFM) and infra-red microscopy (IRM).[151] A recent review by Ruthven et al. describes these various techniques and their application in analysing transport properties.[152] Modelling can also be used to predict diffusivity.[151,153,154] We discuss the analysis of diffusion properties more in detail in section 5.1.6. Regarding thermal properties, as mentioned earlier, there is limited experimental data available on these. This lack of data also makes it difficult to draw a correlation between a material's chemical composition and structural features, and its thermal properties, which in turn hinders the design of sorbents

with the desired thermal properties. Looking at MOFs in general, their thermal conductivities are rather low and this problem could be overcome either by blending them with other materials with higher thermal conductivity, while maintaining their adsorption properties, or by engineering heat exchangers with high contact surface, which could become an expensive solution. Finally, the know-how in terms of manufacturing and post-processing (e.g. pelletisation) to produce ready-to-use sorbents vary significantly depending on the type of sorbent. Zeolites and activated carbons have well-known synthesis routes that have been successfully up-scaled leading to a number of large-scale suppliers around the world. When it comes to more specialised and/or emergent adsorbents like MOFs, the manufacturing and post-processing routes remain active research areas, while a number of manufacturing companies have emerged in recent years.[40] Here, several aspects could be explored: the move from batch to flow processes, the sustainability of the manufacturing step, crystallisation and particle technology fundamentals driving the manufacturing and post-processing steps, the use of additive technology to produce adsorption beds with varied configurations.[155]

4.2.7. Costing processes

Finally, as briefly noted in section 3, in the case of sorbents that are not yet commercialised, their cost often remains an unknown. This can become an issue when comparing sorbents and processes as ultimately, cost is often the main decision driver. As described by Danaci et al.[156], in such situations, two scenarios can be considered: (i) the cost of the sorbent is assumed to be similar to other sorbents currently on the market or (ii) a commercial sorbent is used as a reference. Ultimately though, one would expect a promising sorbent to be manufactured at a scale that would allow reliable estimation of its cost.[156] A recent report proposes a method to estimate the cost of MOF production up to 1 kton per year using MIL-160(Al) as an example.[157] As MOFs move closer to commercial applications, such exercises will likely become more commonplace.

5. Sorbent performance evaluation

As discussed in section 3, process metrics are intimately intertwined with sorption metrics. Thus, the accurate evaluation of sorbent performance is an essential step in the development of an effective separation process. We have highlighted how sorbent performance is primarily evaluated using simple metrics such as working capacity and selectivity, or complex metrics that combine them. In this section, we provide an overview of the methods employed to measure the sorbent performance, both experimentally and computationally. For an exhaustive account on experimental methods, we direct the reader to a recent review by Hu et al.[158] For a thorough analysis of computational approaches, we recommend the equally recent review by Sturluson et al.[159]

5.1 Experimental methods

5.1.1 Single component adsorption isotherms

Collecting single component adsorption isotherms is usually the first step in characterising the adsorption performance of a prospective sorbent. Gas sorption analysers have become widespread in recent years, making gas sorption analysis a routine characterisation method. Gas sorption analysers can be subdivided in two main classes: manometric (often referred to also as volumetric) and gravimetric (Figure 6).[160] Manometric instruments (Figure 6a) measure the pressure change occurring in a calibrated manifold (V_1) once this is brought into communication with a sample cell of known volume (V_2) and equilibrium is reached. Gravimetric instruments (Figure 6b) measure the mass gain of the sorbent when saturated under a given pressure of the desired gas. In both cases, the sample is held at constant temperature using a thermostatic bath. Data are usually provided on a gravimetric basis, i.e. amount of gas adsorbed (in moles, mass or volume STP) per unit mass of sorbent. These data can be expressed in volumetric terms by multiplying times the density of the sorbent. For MOFs, the crystal density is usually employed for the purpose, but it is to be noted that this is the highest theoretical value, as MOF powders are much more loosely packed than a single crystal, and the volumetric capacity is therefore overestimated. Volumetric capacity is less often reported than gravimetric capacity, even though it is the size of the bed, rather than its mass, that defines the costs associated with building the separation plant, contributing to CAPEX, as remarked in section 3. Gravimetric capacity is instead connected with the cost of sorbent, which is usually sold by mass and not by volume, and also impacts on CAPEX.

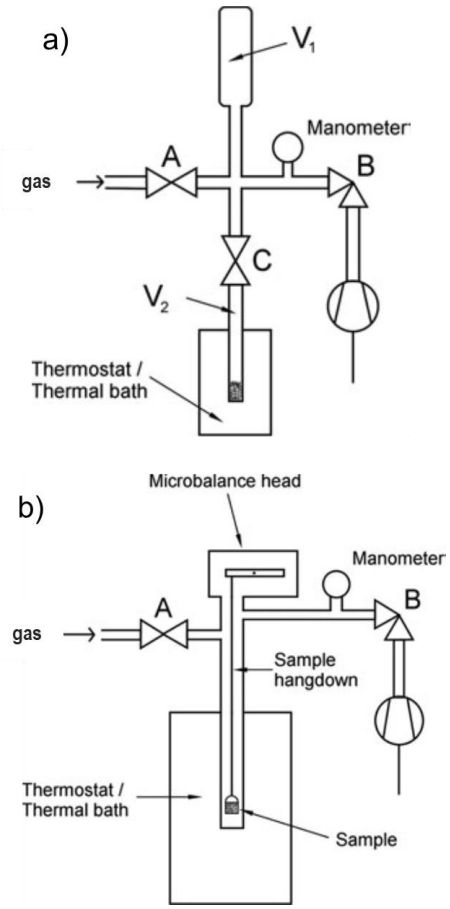

Figure 6. Schematics of isotherm measurement set-ups: a) Manometric/Volumetric, b) Gravimetric. Adapted by permission from Springer Nature: Gas Sorption Measurement Techniques by Darren P. Broom, Copyright 2011.

The amount of sample needed for such measurements can be as low as a few tens of mg, if the MOF under examination has a non-negligible uptake capacity in the pressure range investigated. In principle, measurements can be performed in a range of pressure comprised between 10^{-9} and 100 bar, but the range should be chosen based on the target gas separation, because these analyses can be time intensive. Taking CO_2 capture as an example, if the goal is to test a sorbent for DAC, an instrument able to collect many equilibrium points at pressures in the sub-mbar range is needed, while if the interest is geared towards precombustion capture, the relevant range lies at higher pressures, e.g. 1 to 20 bar. Collecting the desorption branch is also important, because it provides precious information regarding the reversibility of the process, which affects the regenerability of the sorbent. The presence of hysteresis loops in desorption can be especially interesting in this regard, because it might reveal the existence of structural flexibility or kinetic effects in microporous materials.[161,162] Modern instrumentation for gas sorption analysis provides information about kinetics in the form of either pressure drop vs time (manometric instruments) or mass gain versus time (gravimetric instruments). This information can be useful to preliminarily identify diffusion limitations experienced by certain

adsorbates, although a full picture of diffusional properties requires a more thorough approach (see section 5.1.6).

The gas sorption analysers described above not only allow to assess the separation performance of sorbents but can also be used to evaluate their porosity. We note that the models commonly employed to extract textural properties of porous materials, such as specific surface area − e.g. the Brunauer-Emmett-Teller (BET) method[163] − and pore size distribution − e.g. the Horvath-Kawazoe method[164] − from gas adsorption isotherms, usually collected using N_2 at 77 K, were originally derived for "classical" porous materials such as carbons, zeolites or silicas. MOFs often display properties, such as microporosity, multimodal pore size distribution, ultrahigh porosity or flexibility, that challenge the existing models and have stimulated further effort into adapting these methods and developing new ones.[165–171] We emphasise at this point that gas sorption characterisation of a novel MOF should go beyond N_2 adsorption at 77 K, which is often taken as the sole means to define whether a material is porous or not. In fact, a material that displays negligible N_2 adsorption at 77 K might not necessarily be useless for gas separations. At 77 K, N_2 might incur in kinetic limitations that can preclude the system from reaching equilibrium, thus preventing a correct description of the adsorption behaviour in these conditions. Furthermore, other gases might as well not experience the same diffusional limitations in the conditions of temperature and pressure relevant for a separation process. Hence, materials that display negligible BET surface area and pore volume, measured using N_2 at 77 K, and deemed non-porous on this basis, might in fact turn out to be better sorbents than other, more "canonically porous" materials. An example of such a sorbent is a Ca-trimesate coordination polymer that is non-porous to N_2, but upon partial dehydration is able to sieve CO_2 from N_2 and CH_4 and upon complete dehydration can sieve H_2 from CO_2 and C_2H_2.[172,173] Another notable example is CALF-15, based on Zn^{II}, oxalic acid and 3-amino-1,2,4-triazole, which is not porous to N_2 at 77 K, but displays excellent CO_2 adsorption properties.[174,175] As a final remark, we note that positron annihilation lifetime spectroscopy (PALS) can be a valid alternative to reveal the voids in adsorbents whose porosity cannot be probed using standard gas sorption analysis.[176,177]

5.1.2 Dynamic breakthrough analysis

The information obtained from single component adsorption isotherms is ideally complemented by that derived from dynamic breakthrough analysis, which is performed in conditions closer to those of a large-scale separation. A simple, yet comprehensive schematic of a breakthrough analyser is displayed in Figure 7a. The building and running of breakthrough set-up, though simple in theory, require careful considerations and implementation practice. A set of guidelines has been recently summarised in a paper by Wilkins et al.[178] The core of the setup is the adsorption column where the sorbent is packed in either powdered or compacted form. The temperature of the column can be controlled using a thermostatic bath, while the pressure is controlled using a backpressure regulator. For the sake of testing a sorbent for a gas separation, the sorbent bed is exposed to a gaseous stream, typically a binary or ternary

mixture, and the composition of the effluent is constantly monitored with an in-line analytical instrument (most often a mass spectrometer), thus recording the breakthrough profile of each component of the gas mixture. Information about the equilibrium capacity of the sorbent for each species can be obtained by subtracting the integrated area B from A for the light product and integrating area C for the heavy product (Figure 7b).[179] The shape of the breakthrough curve provides information regarding diffusion kinetics: a steep, sharp curve indicates that the adsorption front moves fast through the bed, whereas a broadened curve is indicative of sluggish kinetics. Breakthrough might even occur earlier for a species whose equilibrium capacity is large, but diffuses slowly, than for another species with lower equilibrium capacity but no diffusional limitations, enabling kinetic-based separation.

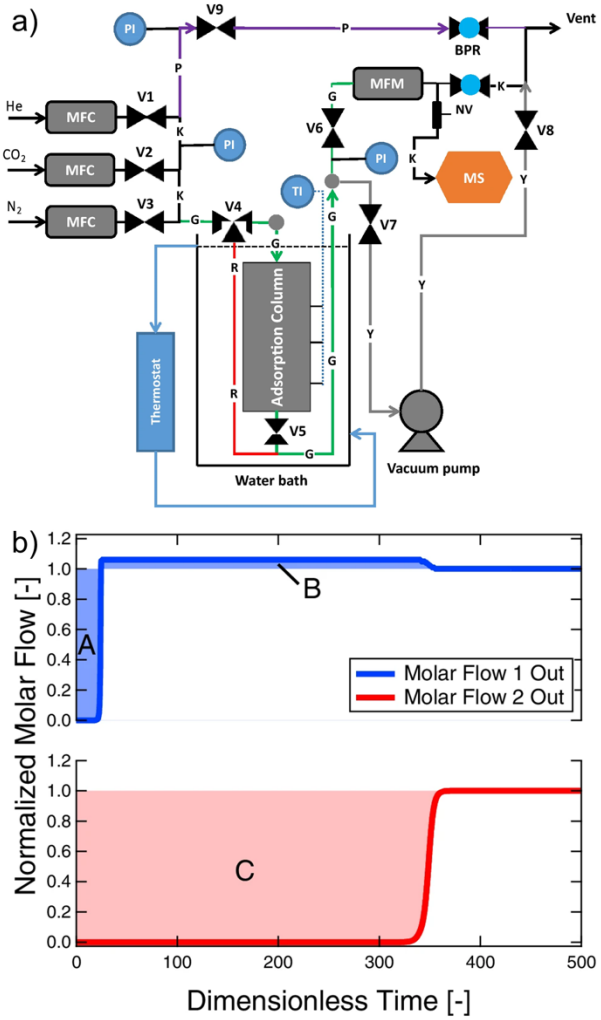

Figure 7. a) Schematic of a breakthrough set-up (Vi = valve, MFC = mass flow controller, MFM = mass flowmeter, BPR = back pressure regulator, MS = mass spectrometer, PI = pressure indicator, TI = temperature indicator). b) Typical breakthrough profiles obtained for the light product (blue) and the heavy product (red) in a multicomponent experiment. Adapted by permission from Springer Nature, Adsorption, 25, 115–133 (2019), “Measurement of

competitive CO_2 and N_2 adsorption on Zeolite 13X for post-combustion CO_2 capture" Wilkins and Rajendran. Copyright (2019). Adapted by permission from Springer Nature, Adsorption, 27, 397–422 (2021) "Dynamic column breakthrough experiments for measurement of adsorption equilibrium and kinetics" Wilkins et al. Copyright (2021).

5.1.3 Working capacity

We have seen in section 3 how working capacity is linked to process metrics such as CAPEX, OPEX and recovery. Therefore, it becomes one of the most important metrics to measure the performance of a sorbent. Determination of working capacity is done in different ways, depending on the nature of the process being PSA/VSA or TSA. In the case of PSA/VSA (Figure 8), the process is often assumed to occur in isothermal conditions and a single sorption isotherm at a given temperature, *T1*, is enough to determine working capacity by simply calculating the difference between the equilibrium uptake at the partial pressure of gas in adsorption conditions (high P) and the uptake at the partial pressure in desorption conditions (low P). The working capacity obtained with this method is the maximum theoretically achievable because a real PSA process occurs in nearly adiabatic conditions, unless heat exchangers are employed, which allow to approach the isothermal regime.[180] The bed temperature will in fact swing between $T1 + \Delta T$ in the adsorption step (exothermic) and $T1 - \Delta T$ in the desorption step (endothermic), thus leading to a decreased gas uptake in the former step and to an increased gas retention in the latter (as remarked in section 3.3).

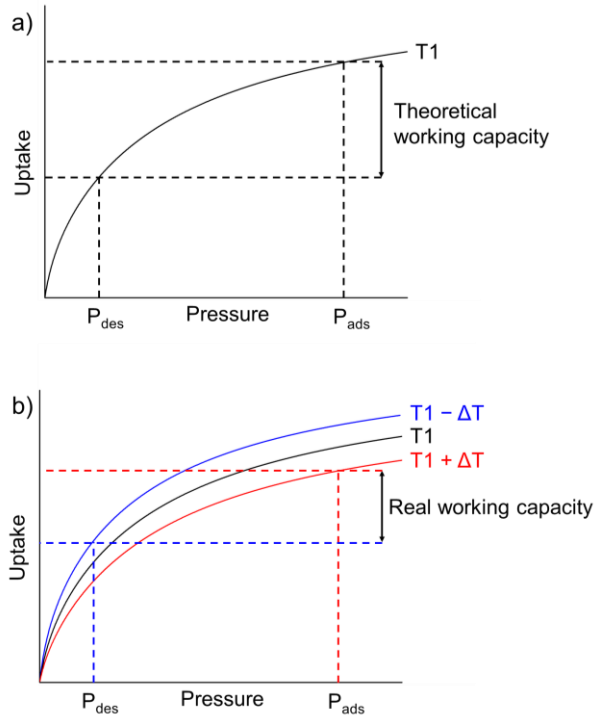

Figure 8. Determination of working capacity for a theoretical PSA process occurring in isothermal conditions (a) and a real PSA process occurring in adiabatic conditions (b) from equilibrium isotherms.

In the case of TSA (Figure 9), working capacity is the difference between the equilibrium uptake at the partial pressure of gas in adsorption conditions (low T) and the uptake at the partial pressure in desorption conditions (high T), therefore isotherms collected at different temperatures are needed. Note that the partial pressure of gas in adsorption and desorption conditions might change significantly. An example is postcombustion carbon capture, where adsorption occurs at 0.04-0.25 bar, while desorption is often taken to occur under an atmosphere of pure CO_2 (1 bar) to avoid dilution of the extract and loss of purity.[181] In this case, adsorption-regeneration cycles can be conveniently carried out using a thermogravimetric analyser (TGA), feeding the desired gas (or gas mixture) at the desired temperature during each stage. This approach is often used to evaluate the performance of amine-based chemisorbents,[182–185] but it has been sometimes applied to MOFs as well.[186–188] TGA can also provide useful information about the kinetics of adsorption and desorption.[189]

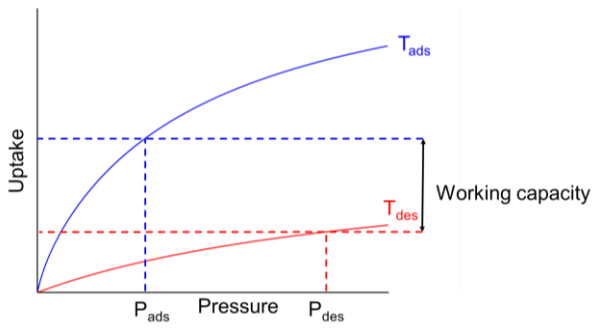

Figure 9. Determination of working capacity for a TSA process from equilibrium isotherms.

5.1.4 Selectivity

Along with working capacity, selectivity also links to process metrics, i.e. purity. The most straightforward way of evaluating the selectivity of a sorbent for a binary separation is through the ideal adsorbed solution theory (IAST).[190,191] At the basis of this approach is the assumption that two gases in a mixture behave as if they were pure (Figure 10). IAST is a simple, yet powerful, tool to predict selectivities that have often been confirmed with other, more sophisticated methods. IAST selectivity can be determined employing user-friendly freeware, such as *IAST++*[192] and *PyIAST*[193] which only require single component isotherm data as an input. However, real gas mixtures can behave in a way that significantly deviates from the ideality assumed by IAST, leading to incorrect estimation of selectivity.[194] For this reason, collecting multicomponent adsorption data is often advocated to obtain accurate determination of selectivity.[195] However, these data require setups that are not yet widely available commercially, such as a breakthrough analyser (see section 5.1.2) or a gas sorption analyser coupled with a gas chromatography system, making multi-component isotherms still rather rare in the literature.[146,194,195]

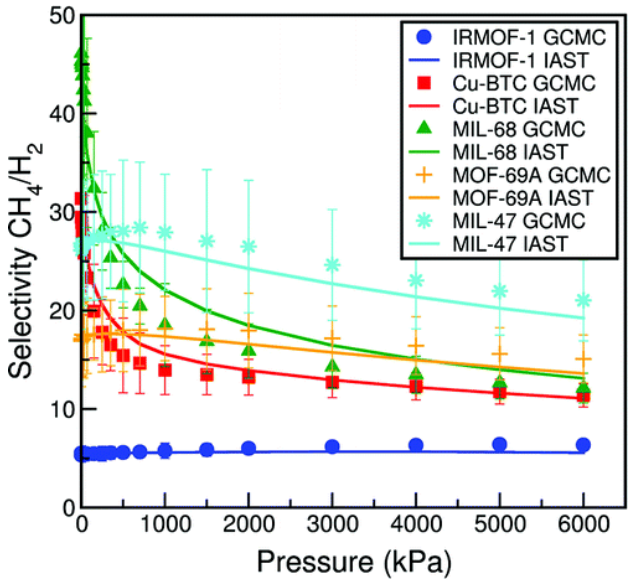

Figure 10. Selectivity for methane from an equimolar mixture of methane and hydrogen as a function of pressure at 300 K for various MOFs. Reprinted with permission from Cessford et al. "Evaluation of Ideal Adsorbed Solution Theory as a Tool for the Design of Metal–Organic Framework Materials", Ind. Eng. Chem. Res. 2012, 51, 13, 4911–4921. Copyright 2021 American Chemical Society.

5.1.4 Heat of adsorption

The value of isosteric heat of adsorption can easily be derived from adsorption isotherms collected over a range of temperatures (ideally at least three different temperatures within 10 °C one from the other) by applying either the Clausius-Clapeyron equation or the Virial equation.[196] Despite being an indirect approach, this is the most widespread method for the determination of heats of adsorption, as it only requires access to a gas sorption analyser to collect the necessary data. Adsorption microcalorimetry, usually performed employing a setup that combines a Tian-Calvet calorimeter with a manometric gas dosing system, provides instead a direct measurement of the heat of adsorption.[197–200] An equilibrium isotherm is measured with such a setup and the amount of heat given off by the sorbent after each gas dose is recorded by measuring the heat flow evolved from the sample cell, compared to an empty reference cell, i.e. the differential heat. The accuracy of the method depends on the accurate determination of both the amount of adsorbate loaded on the surface (derived from the pressure drop in the manometric system) and the heat involved in the adsorption process (derived from integration of the exothermic peak in the differential heat graph). This means that the amount of sample needed for this analysis is usually in the range of a few hundreds of mg, much higher than that required for measuring standard adsorption isotherms. This can render the technique off limits for materials that are difficult to synthesise at that scale, especially at an early stage of development. Furthermore, the need for dedicated equipment makes these measurements still quite rare in the literature. The (isosteric) heat of adsorption is

usually plotted as a function of the gas loading. For most sorbents, the heat of adsorption decreases as the loading increases, because stronger adsorption sites are covered first. At high loading, adsorbate-adsorbate interactions become dominant and the plot approaches the value associated with the heat of condensation of the adsorbate (e.g. 16.7 kJ mol^{-1} for CO_2 at 15 °C)[201]. Reports of sorbents where the heat of adsorption stays constant over a wide range of loading, or even increases, exist in the literature.[175,181] These sorbents usually display uncommon adsorption mechanisms, associated with either cooperative adsorption or flexibility.

5.1.6 Diffusional properties

The importance of characterising adsorption kinetics for the sake of a gas separation has been highlighted in section 4.2.6. Diffusion studies can be subdivided into two main classes: microscopic and macroscopic.[153,154] Microscopic methods include PFG-NMR, QENS, IRM and IFM. These methods can provide detailed information about the diffusional properties at the atomic level, revealing the presence of inhomogeneities, such as surface barriers, that can affect the behaviour of adsorbates. However, these methods require samples with large particle size, possibly single crystals, which are not representative of the powdered sorbents used in a real application. Macroscopic methods, including frequency response, chromatographic methods and ZLC, cannot achieve the level of detail of microscopic methods, but require less sophisticated instrumentation. Most important, they can be applied to realistic samples, providing information that can be relevant for process development. Recently, Karimi et al. reported a volumetric apparatus to simultaneously collect equilibrium and kinetic information.[202] The approach requires mg-scale sample and carefully calibrated vessels.

5.2 Computational methods

5.2.1. Role of computational studies

An approach to evaluate sorbent performance that is being increasingly deployed is the high-throughput computational screening of MOF crystal structures databases in search of candidates with ideal properties for a certain gas separation (Figure 11).[203,159,204] This method involves the simulation of adsorption properties for the desired target gases, with the aim to single out those materials that are predicted to provide the best separation performance, evaluated using metrics such as selectivity, working capacity, energy penalty or composite metrics derived therefrom. The focus of these studies used to be primarily on CO_2 separations,[102,131,205–219] but recent years have seen a broadening in scope, to cover also hydrocarbons separation,[220–222] acetylene purification[91] and Xe/Kr separation.[223–225] These computation-based approaches provide a large amount of information that can, in principle, be very valuable to chemists at the sorbent development stage, allowing to make better decisions about the type of material to target for a certain gas separation. At the same time, the computationally generated isotherms of the selected sorbents could also be fed to process

simulation, to evaluate how those sorbents would perform when employed in a real separation process (see section 4). Then, the focus could be placed on synthesising and testing the sorbents with the best predicted process performance. Thus, computational screenings can provide valuable input for both the process design and the sorbent development stages.

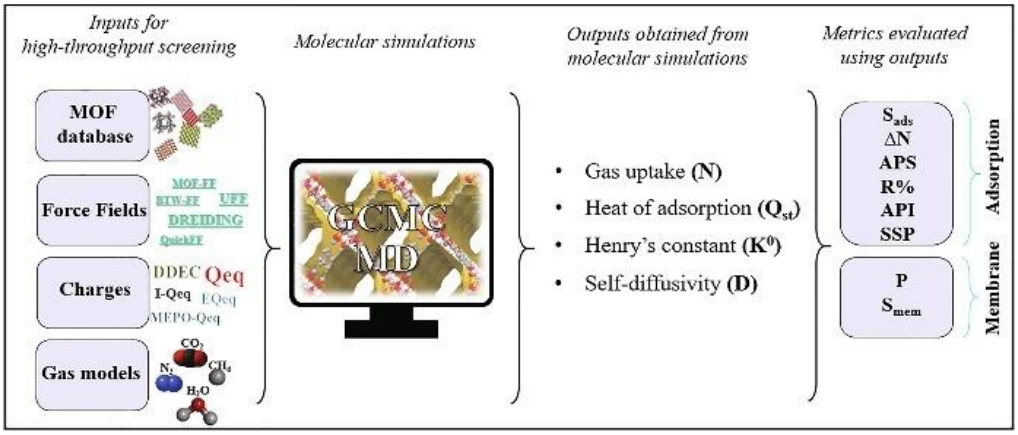

Figure 11. Overview of the high-throughput computational screening of MOF crystal structures to identify candidates with suitable properties for a certain gas separation. Reprinted from Coordination Chemistry Reviews, 422, Hilal Dagla Seda Keskin, Recent advances, opportunities, and challenges in high-throughput computational screening of MOFs for gas separations, 213470, Copyright (2020), with permission from Elsevier.

Computational screenings of MOFs for applications in gas separation and storage started appearing in the literature in the late 2000s, taking advantage of the increasing accessibility of computational power.[206,208,226] The main motivation behind the development of these methods is that the number of existing and potentially synthesisable MOFs is too large to be effectively screened experimentally for each and every potential application.[227] The idea to feed a computer with MOF structures and get a pool of materials with exceptional separation performance in return is in fact very attractive for an experimental chemist seeking a precise direction to focus their synthetic efforts on.

5.2.2. Overall approach

Computational screenings are either performed on databases of known MOFs (CoRE MOF[126,127] and CSD MOF subset[124,125] are the most common) or on databases of hypothetical MOFs (such as those developed by Snurr and Wilmer,[228] the Tobacco database,[229] the one developed by Woo[230]). In these works, the main goal is to screen a large number of candidates and to identify trends in terms of storage/separation performance on the basis of certain structural or chemical descriptors. Adsorption isotherms are usually predicted based on GCMC simulations, which are less computationally demanding than quantum mechanical calculations, but might not necessarily be representative of real isotherms, because simulations often overlook preferential interactions with certain structural units (e.g. open metal sites) and possible non-

Langmuir behaviour (see section 6.2), due to the common assumption that the framework is rigid.[159]

These screening studies work well for storage applications, where only one species is involved in the adsorption process and this species is usually either methane, hydrogen or, less often, oxygen, which have weak, non-specific interactions with the sorbent due to their low dipole moment, quadrupole moment and polarisability.[228,231–234] Therefore, several works have converged towards the conclusion that the storage performance at high pressure correlates well with geometric descriptors, such as surface area, pore volume, largest cavity diameter (LCD) and pore limiting diameter (PLD), whereas framework chemistry has a less prominent role.

Gas separation features additional complexity: there are at least two species involved, which can even compete for the same adsorption sites, the partial pressure of the species of interest is often in a range where framework chemistry bears an important influence on the adsorption behaviour, and separation can occur via different mechanisms, as discussed in section 2. Therefore, simple geometric descriptors do not provide a full picture. One of the classical problems encountered is the presence of open metal sites, which require that partial charges be assigned and specific force fields be used to accurately describe the adsorbate-site interaction and produce an isotherm that is faithful to the experimental one.[235–237] These screenings do not capture materials where reactive gas adsorption might occur either, which can be important when CO_2 is involved (e.g. formation of carbamates between amines and CO_2[181,186] or formation of bicarbonates between hydroxide and CO_2[238]). Furthermore, they do not consider potential flexibility of the framework, which could lead to selective uptake of certain species able to trigger a specific structural response. Being based on equilibrium isotherms, potential for kinetic separation is rarely accounted for. This is especially important for olefin/paraffin separation, where thermodynamics-driven separations are not always possible due to similar interactions of the adsorbates with the framework, as remarked in section 2.2.9.

5.2.3. Limitations and challenges

After ten years of deployment of large-scale computational screenings, what input have these methods given so far, in terms of materials discovery for gas separations? This question can be broken down into two sub-questions. The first is whether mining databases has led to "rediscover" materials that are known to perform well for certain gas separations. To answer this question, we can use post combustion CO_2 capture as an example, for the simple reason that the majority of these studies have targeted this application, as already noted in the previous section. Some MOFs based on inexpensive metals, simple linkers and that have experimentally been proven to be good candidates for this separation are UTSA-16[239,240] (CSD refcode RAZXIA), IISERP-MOF-2[241,242] (CSD refcode ACICOH), CALF-15[174,175] (CSD refcode MUDKOM) and SIFSIX-2-Cu-i[243] (CSD refcode YEMTIV). To the best of our knowledge and based on the available literature to date, none of these materials have ever been identified by any

high-throughput computational screening reported in the open literature. What could be the reason? Are these MOFs not part of the databases employed to compute adsorption properties? A simple search in the CSD MOF subset reveals that all refcodes are present in the list. UTSA-16 and CALF-15 are also included in the CoRE MOF database. Perhaps there are in fact MOFs with much better potential than them? Or maybe the models are still not able to give us realistic results? The second question is whether screening databases of hypothetical MOFs has enabled identifying candidates that have been experimentally demonstrated to display superior performance to benchmark materials. The answer to this question is not a simple one. While, as previously mentioned, examples of record-breaking computationally designed MOF sorbents for gas storage have been reported, the same has not happened for gas separations yet. The reason behind this lies, again, in the increased complexity of a separation process compared to a storage one: a material for gas storage is judged on the basis of well-defined parameters, such as gravimetric and volumetric deliverable capacity, whereas the success of a separation process is measured in terms of recovery, purity and cost, which are not characteristics proper of the sorbent material, rather of the sorbent-process combination, as highlighted in section 3.

Despite the limitations discussed above, computational screenings have produced precious information, especially in terms of identifying bad performers and unavoidable performance limitations. Most studies converge towards the conclusion that, in purely structural terms, there is an ideal range of pore size for each separation: smaller pores might improve selectivity, but are detrimental to working capacity, while larger pores afford higher working capacity, at the expense of selectivity. If the pore size is too large, effective interaction between sorbent and adsorbate is lost and adsorbate-adsorbate interactions become dominant, with negative impact on the ability of the sorbent to be effective at low partial pressures.

Given the necessary approximations needed to screen very large pools of candidates, it would perhaps be better to focus on certain subsets of MOFs to limit the number of candidates and increase the level of accuracy of the simulation. For example, one could focus only on MOFs with pore size lower than 10 Å, MOFs with channel-like pores, MOFs based on a certain class of linkers, or MOFs based on earth-abundant metals. A good recent example in this direction is the work of Sholl and co-workers,[223] who have constructed a database of 936 anion-pillared materials, analogues of the SIFSIX family, and screened them for Xe/Kr separation, identifying a promising candidate not yet experimentally reported. Snurr and co-workers[121] used instead the cost of the metal as a discriminating factor, removing from the CoRE MOF database all the MOFs where the cost of the metal exceeds $40/(kg of MOF).

6. MOF sorbent design and development

Having provided an overview of how a separation process is designed and its performance evaluated, how the performance of the sorbent alone is evaluated and how the sorbent's

performance influences process design, we now proceed to analyse the MOF sorbent development step. The output of both process simulation and sorbent performance evaluation can become a precious input for material chemists seeking to develop novel MOF sorbents for a specific gas separation. This task can be accomplished either by rationally designing an entirely new MOF with the desired properties or by "repurposing" an existing MOF with suitable properties that was not previously considered for that specific application.

6.1 MOF design

Ever since the inception of the field of MOFs, the concept of rational design has been a central one, given the modularity of their crystal structure and the ease in predicting topological properties by combination of inorganic secondary building units (SBUs) and organic linkers with well-defined geometrical features (Figure 12).[31,244,245] The crystalline nature of most MOFs has played a central role in enabling the development of reticular chemistry and the ever-increasing number of MOF structures deposited in the CSD is a testament to the success of this approach.[124] The field was initially dominated by the race to record high surface areas and pore volumes, which heavily relied on the principles of reticular chemistry to expand the pore size of some families of MOFs based on certain building blocks and underlying topologies.[245–248] This trend has well served the purpose of demonstrating the potential of reticular chemistry but has progressively been replaced by more application-driven approaches that focus on fine tuning structural and physicochemical features to endow the material with the desired function.[249–251]

As far as gas separations are concerned, an ideal MOF sorbent must combine a number of features that can satisfy the process demands, as highlighted in the previous sections: high working capacity for the desired species, low working capacity for undesired species, high selectivity, fast kinetics of adsorption and desorption, high stability and low cost of manufacturing.[8] The performance of a MOF in a gas separation is linked to both inherent and emergent properties (see section 3): chemists have become very skilled in precisely tuning the inherent properties through rational design, while the relationship between these and emergent properties still escape a complete understanding, and therefore a truly rational approach to tune emergent properties is still lacking. Common strategies to increase the affinity of a MOF for a certain species include creating open metal sites - which provide enhanced interaction with polar and quadrupolar species - functionalising the organic linker with groups displaying Lewis acidity (e.g. hydroxyls, carboxylates) or basicity (e.g. amines, amides), finely tuning the pore size and shape to maximise the contact surface between adsorbate and pore walls. The use of these approaches to design MOFs for a wide range of gas separations has been extensively reviewed in the literature.[37–39,41,90,252,253]

Besides adsorption properties, stability plays a central role in determining the success of a MOF sorbent in a real-life application, as remarked in section 3.6.[254–260] The MOF must be able to withstand temperature changes, chemical attack and mechanical stress without dramatic

reduction of its performance over its lifetime in the adsorption column. Thermal and chemical stability can be maximised by strengthening the coordination bonds between metal and linker, which have been recognised as the weakest part of the structure. This can be achieved by choosing metals with high oxidation states, i.e. +3 (Al, Fe, Cr) and +4 (Ti, Zr),[257,261] and/or by using organic linkers with soft Lewis bases, such as azolates,[256,262–266] or stronger coordinating groups than carboxylates, such as phosphonates,[267,268] which can afford stable structures also with divalent metals. Mechanical stability is instead mainly governed by the underlying topology and displays a positive correlation with density as well.[259,269] The dimensionality of the inorganic units also bears an important influence on the stability of a given framework: in moving from 0-D clusters to 1-D chains to 2-D layers, the stability usually increases.[270] A good example in this regard is the case of UiO-66[271] and MIL-140A,[272] both based on Zr^{IV} and terephthalate but assembled upon different inorganic units: UiO-66 contains hexanuclear Zr^{IV} oxoclusters, whereas MIL-140A contains polymeric chains composed of Zr^{IV} ions linked via oxo anions and carboxylates. MIL-140A is in fact more stable than UiO-66, both chemically, thermally, and mechanically.[272]

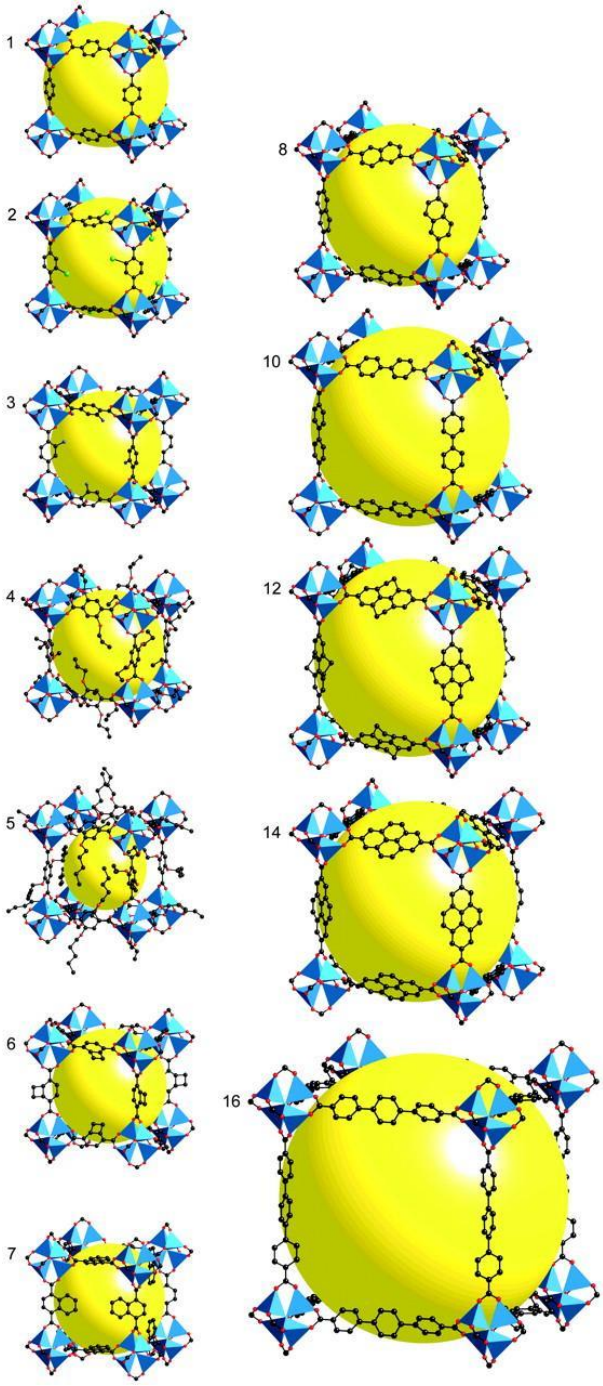

Figure 12. Examples of isoreticular MOF (IRMOFs) structures based on the same SBU of formula $[Zn_4O(OOC)_6]$ and with varied linker's length and/or functionality. From Eddaoudi et al. "Systematic Design of Pore Size and Functionality in Isoreticular MOFs and Their Application in Methane Storage" Science 2002, 295, 469-472. Reprinted with permission from AAAS.

Lastly, cost considerations should be done when picking a metal and a linker to design a MOF, given the importance of the sorbent cost in the economics of a separation process. The metal component deserves particular attention, as its cost is highly dependent on its natural

abundance and on the ease to source it. An example of an abundant, yet relatively expensive, metal is zirconium, whose concentration in the Earth's crust is about twice that of nickel, zinc or copper,[273] but whose production depends on the mining and processing of the titanium minerals ilmenite and rutile, as well as tin mining.[274] Another important aspect is the metal's toxicity, which should lead to rule out elements like cadmium and lead. Ideally, rock forming elements (Ca, Mg, Al, Fe, Ti) should be privileged, because of their abundance, low cost and low toxicity. On the linker side, care should be taken to select species that are related to existing industrial production processes, such as polymer precursors, or can be derived from biomass feedstock.[119,275–277]

6.2 Ultramicroporous MOFs

The excitement initially aroused around the ultrahigh surface area and porosity of MOFs drove research into their use as gas storage media. With time, it has progressively become evident that an effective MOF sorbent for a gas separation needs not having large pores, but pores with size and shape that either allows intimate interaction between a specific adsorbate and the surface (equilibrium separation) or prevents one species from freely diffusing (kinetic separation/sieving) to increase selectivity. This realisation has led, in recent years, to shifting the focus towards the development of ultramicroporous MOF sorbents (i.e. with pore size < 8 Å) with precisely tailored pore structure and chemistry, leveraging on the principles of reticular chemistry and crystal engineering.[39,41,278,279] The most straightforward approach to prepare ultramicroporous frameworks involves the use of short linkers, such as, for example, oxalic acid,[174] fumaric acid,[280,281] squaric acid,[95,282] isonicotinic acid,[241,242] pyrazine.[243] In this context, the phenomenon of framework interpenetration,[283–288] once considered a nuisance because responsible for reduced surface area and pore volume, has also been reconsidered as a useful method to control pore size in ultramicroporous MOFs.[243]

Ultramicroporous MOFs usually display relatively low surface area and pore volume, which limits their saturation uptake capacity (and therefore the working capacity), but their density is higher than the average MOF, which makes their volumetric capacity competitive with more porous sorbents. Furthermore, thermal conductivity is enhanced in denser materials,[108,109] which is beneficial especially for TSA processes, as remarked in section 3. Another point of interest, also mentioned in section 6.1, is that denser frameworks tend to be more mechanically resistant than highly porous ones, which becomes important both at the stage of shaping powders into compacted forms and during operation, when the pellets are subject to attrition and friction. In fact, most of the MOFs displaying promising performance for several separations are ultramicroporous.[41,279]

The SIFSIX family and related compounds (TIFSIX, NbOFFIVE, etc.), often referred to as "hybrid ultramicroporous materials" are a representative example of a class of ultramicroporous frameworks that, upon their rediscovery a few years ago (the synthesis and crystal structures of

some prototypical members were first reported 20+ years ago),[289,290] have been intensively engineered for several gas separations, including post combustion CO_2 capture,[243] direct air capture,[291–293] natural gas upgrading,[294] acetylene purification,[89] C_2 hydrocarbons separation.[295,296] These MOFs are constituted of layers of divalent metal ions (e.g. Cu^{II}, Zn^{II}, Ni^{II}, Cd^{II}) connected through heterocyclic organic bridging linkers (e.g. pyrazine, 4,4'-bipyridine), with inorganic fluorinated anions (e.g. SiF_6^{2-}, TiF_6^{2-}, AlF_5^{2-}, $NbOF_5^{2-}$) acting as pillars (Figure 13).[297] The combined presence of fluorinated inorganic anions and ultrasmall channel-like pores is key to generate a favourable environment for species with large quadrupole moment and/or polarisability. This is well reflected by the high heats of adsorption typically observed for these sorbents, even though covalent bonds are not involved in the adsorption process. In addition, the possibility to fine tune the pore size to the sub-Ångstrom level allows to achieve kinetic separation and molecular sieving. Efforts have been made in assessing the effect of systematically changing every component of the structure, be it metal, organic linker and/or inorganic pillar, on the pore size and chemistry, leading to identify materials with excellent separation performance and stability. There are several other examples of interesting ultramicroporous MOFs that could be mentioned, but a comprehensive account goes beyond the scope of this work. We refer the interested reader to some recent authoritative reviews.[39,41,278,279]

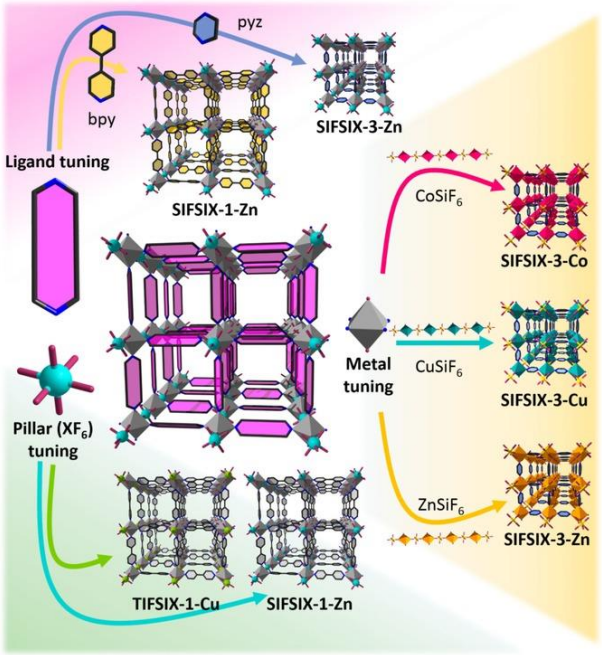

Figure 13. Tuning of the various components of the framework of ultramicroporous MOFs belonging to the SIFSIX family. Reprinted from Chemistry, 23, Guillerm et al., "Continuous One-Step Synthesis of Porous M-XF_6-Based Metal-Organic and Hydrogen-Bonded Frameworks", 6829-6835, Copyright (2017), with permission from John Wiley and Sons.

6.3 Flexible MOFs

One of the most peculiar features of MOFs, compared to other adsorbents, is their structural flexibility, which can be induced by various external stimuli, such as guest insertion, temperature, pressure, electrical fields.[298,299] Adsorption-driven flexibility in MOFs can take different forms (Figure 14): framework expansion ("closed" phase to "open" phase transition, e.g. in Co-bdp[300]), swelling ("closed" to "open" transition with no change in pore shape, e.g. in MIL-88[301–303]), framework contraction ("open" to "closed" transition, e.g. in DUT-49[304–306]), breathing ("open" to "closed" to "open" transition, e.g. in MIL-53[162,307]), subnetwork displacement (e.g. in ELM-11 and ELM-12[308,309]), linker rotation (e.g. in ZIF-8[310]).

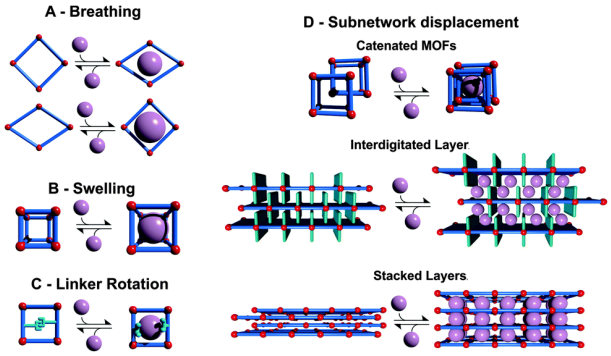

Figure 14. Overview of common types of flexibility encountered in MOFs. Reproduced with permission from ref. 264.

These flexible materials do not display the classical Langmuir-type adsorption behaviour, but step-shaped isotherms, indicative of adsorption of large amounts of gas in a narrow range of pressures once a threshold pressure is reached (Figure 15).[162,311] If the phenomenon is triggered by only one of the species in the mixture in working conditions, the MOF will be endowed with excellent selectivity. We remark that pore opening upon adsorption of the target species might also lead to improved adsorption of the undesired species, thus impacting selectivity.[312] In this case, simple application of IAST to single component isotherms is not sufficient to predict whether co-adsorption will occur,[313,314] and breakthrough analysis becomes crucial to obtain experimental evidence of selectivity. Step-shaped isotherms potentially allow for large working capacity upon a small pressure or temperature swing, with reduced energy demand for regeneration.[181] However, hysteresis in desorption is often observed in these systems, which mitigates the potential benefits, in terms of working capacity, of having a sorbent switching from an "empty" state to a saturated one over a small range of pressures. Hysteresis typically appears in sorbents that undergo large volume changes associated with adsorption and desorption.[299] This behaviour can hamper practical implementation of some flexible sorbents in pelletised form, due to the mechanical stress caused on the pellets by cyclic expansion and contraction.[315,316]

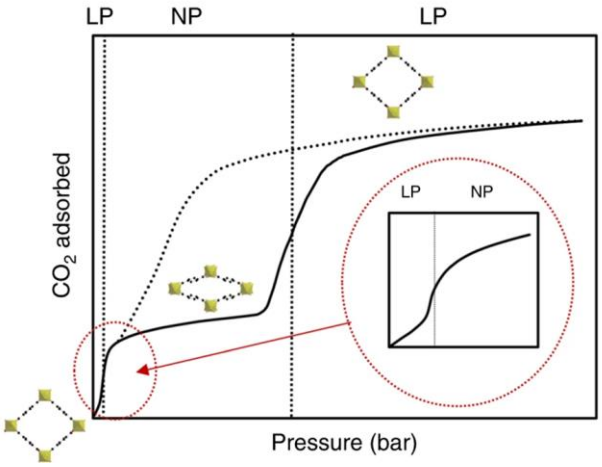

Figure 15. Hysteretic step-shaped CO_2 adsorption isotherm in the breathing MOF MIL-53. Reproduced with permission from ref. 275.

Another practical challenge is linked to the shifting of the step-shaped isotherm to higher pressures at higher temperatures (and vice versa): due to the exothermic nature of adsorption and to the low heat capacity of MOFs, the bed temperature can significantly increase. If a temperature is reached at which the step occurs above the partial pressure of the target gas, the sorbent might be unable to retain the adsorbate, losing its effectiveness. However, major structural rearrangements often have relatively high activation barriers, meaning that part of the heat evolved during adsorption is reabsorbed by the sorbent during the phase transition. Such intrinsic heat management can reduce the temperature increase and thus mitigate the effect of the shift of the isotherm.[300,317] Finally, it is worth to note that sorbents exhibiting step-shaped isotherms may also display breakthrough curves with unusual shapes, resulting from the combination of multiple shock waves.[318] These uncommon breakthrough curves can also pose challenges to practical implementation, although solutions to mitigate the issue are appearing in the literature.[317]

In terms of rational design, flexible frameworks are less straightforward than rigid ones, and research advances in this direction have mainly stemmed from serendipitous discoveries, followed by intense experimental and computational work aimed at understanding the origin of the flexible behaviour.[319–321] As an example of the scarce predictability of flexible behaviour, we can cite the classical breathing MOF, MIL-53(Al) (based on terephthalate linkers),[162,307,322] whose analogues based on the shorter linker fumarate (commercialised as Basolite A520 by BASF),[281] and on the longer linker 4,4'-diphenyldicarboxylate (known as DUT-5)[323] do not display flexibility. It has recently been suggested that some topological nets might be intrinsically foldable, providing a potential blueprint for designing flexible MOFs from scratch.[324] In a similar vein, large scale computational screening of crystal structure databases is but a trivial task:[159] these materials are intrinsically dynamic and crystal structures can only capture the average of a structure that may or may not be dynamic. In order to describe these

dynamics, more expensive calculations have to be deployed, which are not applicable to a large number of candidates.

Even flexibility on a local scale, which does not impact on the sorbent's volume (e.g. libration motion of aromatic rings, thermal vibration)[325], can bear a significant influence on the adsorption behaviour, as demonstrated by Smit and coworkers for the case of Xe/Kr separation.[326] In MOFs with predicted poor performance based on a rigid approximation, flexibility can improve selectivity for one adsorptive by allowing diffusion through pores that have rigid diameter smaller than the kinetic diameter of that adsorptive. However, in MOFs with predicted good performance, flexibility can be detrimental for selectivity by affecting the optimal interaction between sorbent and guest predicted based on the rigid approximation. SBMOF-1[327] is an example of a MOF that displays lower experimental selectivity than the predicted one,[225] a phenomenon attributed to local flexibility, according to Smit and coworkers.[326] Agrawal and Sholl[328] further extended work in this direction by including species with non-spherical shape (i.e. CO_2, ethane, ethene, propene), finding that some separations are more affected than others by flexibility and that MOFs with smaller pores (LCD < 6 Å) can undergo larger changes than MOFs with larger pores, mainly in terms of selectivity. This aspect has only been assessed very recently, computationally but also experimentally,[325,329] so we still have little understanding of local flexibility. Therefore, at present we have very limited control on this phenomenon at the design level.

6.4 Hypothetical MOFs

A wealth of computational approaches have been deployed to generate libraries of hypothetical MOFs (hMOFs), inspired by the work done on zeolites.[229,230,330–335] The most common strategies are either the so-called "tinker toy" approach, proposed by Snurr and co-workers,[331] or topological-based methods.[229,230,332] Regardless of the chosen method to construct the framework, hMOFs have mainly been generated based on a few commonly occurring SBUs (e.g. $[Cu^{II}_2(OOC)_4]$ paddlewheel, $[Zn^{II}_4O(OOC)_6]$ octahedra, $[Zr^{IV}_6O_4(OH)_4(OOC)_{12}]$ clusters), while mainly intervening on the backbone of the organic linker (Figure 16). Since SBUs are 0-D clusters, the resulting frameworks usually feature spherical pores, whereas structures with channel-like pores, usually based on 1-D rod-shaped units, tend to be underrepresented. In some instances, promising materials were identified, mainly for gas storage applications, synthesised and experimentally validated.[331,336–338]

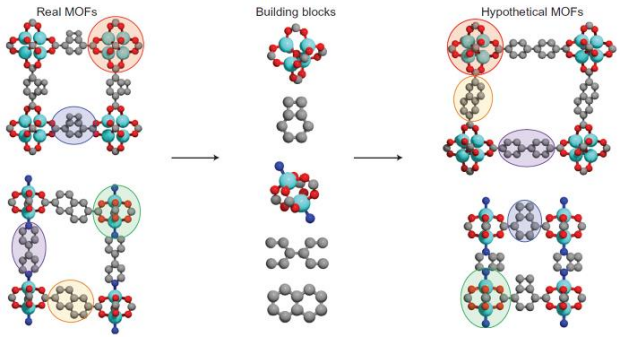

Figure 16. "Tinker-toy" approach to construct hypothetical MOFs based on well-defined inorganic SBUs. Reprinted by permission from Springer Nature: Nature Chemistry 4, 83–89 (2012) "Large-scale screening of hypothetical metal–organic frameworks", Wilmer et al. Copyright (2012).

One of the main issues that has been recognised in these databases of hMOFs is their lack of diversity:[339] they usually only consider a limited number of SBUs and almost exclusively carboxylate linkers. Such an approach neglects the huge chemical and topological space potentially accessible when other metals or other inorganic units containing the same metal are concerned, as well as other coordinating groups than carboxylates. Other types of linkers, such as azolates and phosphonates, are much less experimentally investigated than carboxylates, although they could offer opportunities to access frameworks displaying new structures and even new adsorption mechanisms.[262,267] The emphasis on carboxylate-based structures is mainly due to their higher predictability, thanks to the well-established SBU approach. As an example, out of the MOFs known to perform well for post-combustion carbon capture and mentioned in section 5.2 (UTSA-16, IISERP-MOF-2, CALF-15, SIFSIX-2-Cu-i), none is based on a common SBU. Furthermore, computationally generated structures often imply the usage of complex organic linkers that can feature multiple functional groups.[335,340] There is no guarantee that these linkers can be effectively prepared in a straightforward manner. Even in the case of hMOFs based on apparently simple linkers, such as dihydroxyfumaric acid, identifying the appropriate conditions for the formation of the desired framework is but trivial.[341] Algorithms to assess the effective synthesisability of these hypothetical MOFs are being developed, which should help in rapidly discriminating realistic targets from impractical ones.[342] Computational tools have also recently been used to mimic the chemical intuition of an experimentalist, which can use the results of unsuccessful experiments to identify the best conditions for MOF synthesis.[343] However, at present this evaluation mainly rests in the hands of an experienced experimentalist, meaning that it is necessary that computational chemists and synthetic chemists establish a dialogue, if we are to accelerate materials discovery using this approach.

The recent work of Smit et al.[337] is an excellent example of how such a synergy can lead to significant advancements. The target application in this work is postcombustion carbon capture in humid conditions. They built a database of 325000 hMOFs expanding the range of inorganic units to include also 1-D, rod-shaped units based on V^{III}, Ba^{II} and Al^{III}, which generate structures

with channel-like pores having uniform size. Among them, 8352 were found to combine working capacity and selectivity higher than those of zeolite 13X in dry conditions. An analysis of the CO_2 binding sites revealed that there were three main classes: two parallel aromatic rings with interatomic spacings of approximately 7 Å (31% of all binding sites); metal–oxygen–metal bridges (32%); open metal sites (21%). These materials were screened for their affinity for water, finding that those featuring the first class of adsorption sites display lower Henry coefficient for H_2O. Two Al^{III}-based MOFs were selected, synthesised and experimentally demonstrated to be able to selectively adsorb CO_2 in the presence of H_2O, as predicted by computations.

6.5 Ab initio design of MOFs

The construction of hMOFs is purely based on structural considerations, without providing information on what synthetic conditions can afford the desired hMOF. Yet, hMOFs considered promising for a certain application have been successfully prepared in various instances. This has been possible mainly thanks to the empirical knowledge of the conditions needed to favour the formation of the common SBUs mentioned in section 6.4. Little work has been done instead in the direction of predicting *ab initio* what structures can be generated from a given combination of metal and linker.[344–351] This is likely due to the scarcity of experimental evidence and fundamental understanding of how building units self-assemble during synthesis and what synthetic parameters can steer the process towards one specific structure rather than others.

As an example of the complexity of self-assembly processes, we can use the case of coordination polymers based on Co^{II} and 1,3-benzenedicarboxylate (isophthalate), one of the simplest and least expensive carboxylates. The recently reported MUF-15[352] (Figure 17), based on these two species, displays inverse C_2H_6/C_2H_4 selectivity, a highly sought-after feature (see section 2.2.9), and can be prepared in a simple way in water/methanol solvent. Thus, MUF-15 can be seen as a typical low-hanging fruit. Why wasn't it discovered earlier then? A search in the CSD for the crystal structures of compounds containing Co^{II} and isophthalate as the sole organic linker leads to identifying nine more entries appearing in the literature between 2001 and 2013, long before MUF-15 was discovered.[353–359] So, even though the same reagents had been the object of rather intense investigation, no one had identified the synthetic conditions to obtain MUF-15. Curiously, a nearly identical compound to MUF-15 was reported, but its gas adsorption properties were not assessed.[355]

This example highlights two important points: first, the variety of structures accessible with simple linkers by tuning the reaction conditions is wide and strongly dependent on which way the inorganic part of the framework assembles; second, not all low-hanging fruits have been harvested yet, leaving room for the future discovery of MOFs built from readily available linkers that, like MUF-15, offer attractive gas separation performance. Some works have shown that the role of the solvent in this context is crucial, as it can even coordinate to the metal and assist

the assembly process.[360–363] Shedding light on this aspect should be the focus of future investigation.

Another challenging task is to foresee whether a framework will interpenetrate or not. The challenge is two-fold: first, one has to predict what topologies are accessible using certain building blocks and whether these can lead to interpenetration or not (e.g. dual and self-dual nets are likely to interpenetrate,[285,364] whereas frameworks based on rod-shaped (1-D) or layered (2-D) inorganic units are less likely to do so)[365], second, the right synthetic conditions must be identified that afford the framework with the desired degree of interpenetration.[288] Given the importance of interpenetration to fine tune the pore size, this is an area where fundamental understanding is crucial to achieve true rational design. Finally, the effect of defects, now universally acknowledged to exist in many frameworks, is another feature that we are not currently able to properly simulate, predict and describe.[366,367] Yet, researchers are learning how to harness defects to tune the physical-chemical properties of MOFs, including their adsorption behaviour.[368,369] All these aspects still escape a proper computational-based treatment and are therefore mainly left to experimentation.

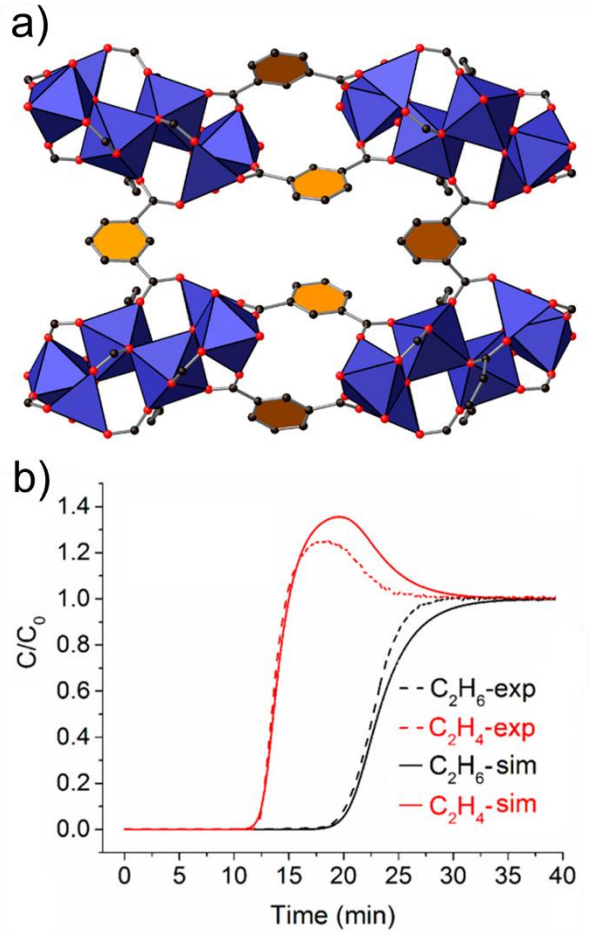

Figure 17. Polyhedral representation of the crystal structure of MUF-15 (a) and comparison of experimental and calculated breakthrough curves for C_2H_4 and C_2H_6 (b). Reprinted (adapted) with permission from Qazvini et al. "A Robust Ethane-Trapping Metal–Organic Framework with a High Capacity for Ethylene Purification" J. Am. Chem. Soc. 2019, 141, 12, 5014–5020. Copyright 2021 American Chemical Society.

6.6 High-throughput synthesis

Given the current limitations of computation-assisted MOF design seen in sections 6.4 and 6.5, discovery of new materials can still be accelerated by deploying high-throughput experimental methods.[145] This "brute force" experimental approach was initially employed to the synthesis of zeolites in the late 1990s[370] and spilled over to the field of MOFs not long afterwards.[371,372] The method involves the use of parallel reactors, typically based on the 24, 48 or 96 well-plate formats, whose volume can vary from the µL to the mL scale. Accurate reagents dispensation is crucial when dealing with such small volumes and is usually ensured by the use of automatic dispensing units. Syntheses can be carried out using conventional heating, microwave-assisted heating or ultrasonication.[373] In order to avoid bottlenecks downstream of the parallel synthesis step, the many MOF samples produced should also be worked up and characterised at a basic level (i.e. X-ray diffraction) in a high-throughput manner.

The workflow in this case requires to first define some guiding design principles and identify the desired building blocks, and then deploy high-throughput parallel synthesis methods to considerably reduce the time needed to explore the parametric space. This is especially beneficial when dealing with metal-linker systems that can give rise to a multitude of different products upon small variations of the synthetic parameters. The complexity of some parametric spaces, such as that of the Co^{II}-succinate system studied by Cheetham and co-workers,[372] is such that a conventional serial approach would require a huge investment of the chemist's time to be mapped in a comprehensive manner. The Co^{II}-isophthalates discussed in section 6.5 would also be an ideal case study in this context.

Recently, big leaps forward have been made in using robots to carry out synthetic work, with the promise of bringing automation in the chemistry laboratory.[374] This could improve reproducibility of results and relieve the experimental chemist from the burden of performing repetitive tasks, allowing them to focus on intellectual activities.

6.7 Reinventing the wheel

Given the already huge pool of existing MOF structures, rational design "from scratch" can be accompanied by *ex post* rediscovery of candidates already existing in the CSD. With almost 100000 crystal structures reported, there is certainly scope for spotting MOFs that can offer attractive gas separation properties but have never been characterised with this application in

mind. In section 5.2, we have seen how computational screenings have been extensively used to mine databases of MOF structures with this purpose. At the same time, the ability of experienced experimentalists to recognise a material with the right features for a certain gas separation application has also produced some remarkable results. We previously mentioned the case of SIFSIX-type materials, which were found to display outstanding gas separation properties more than a decade after their first appearance in the literature.[289] [108] One of the most promising sorbents for postcombustion CO_2 capture available these days, UTSA-16, based on the readily available citric acid as the linker and Co^{II} and K^{I} as the metal ions, was first reported in 2005 and initially only studied for its magnetic properties.[239] It took seven years before its potential as a highly selective sorbent for carbon capture was revealed in 2012.[240] Another textbook example is the case of a material based on Ca^{II} and squaric acid first reported in 1987[282] – well before the acronym "MOF" was coined – which was recently rediscovered by Banglin Chen and coworkers[95] to display outstanding performance in separating ethylene from ethane via molecular sieving (Figure 18). The same material (rebranded UTSA-280) has subsequently been demonstrated to be able to sieve CO_2 from CH_4[375] and to display record Kr/Xe selectivity.[376] An important feature of this MOF is also that it can be easily synthesised at room temperature in aqueous medium starting from commercially available reagents, even on a relatively large scale.[95] It is perhaps appropriate to note here that another work, published almost simultaneously, reports a somewhat less impressive performance of the same sorbent for ethane/ethylene separation.[377]

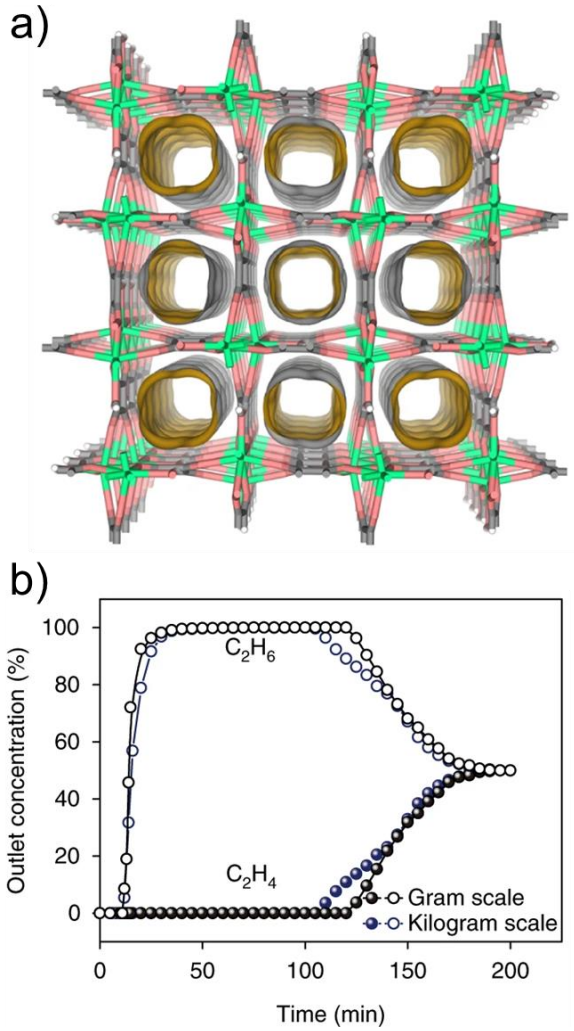

Figure 18. Crystal structure of UTSA-280 (a). Colour code: Ca, green; O, red; C, gray; H, white. The yellow contour plots represent the accessible surface. Comparison of breakthrough curves for C_2H_4 and C_2H_6 obtained using the MOF prepared on a gram scale and on a kilogram scale (b). Reprinted (adapted) by permission from Springer Nature: Nature Materials, 17, 1128–1133 (2018) "Molecular sieving of ethylene from ethane using a rigid metal–organic framework", Rui-Biao Lin et al. Copyright (2018).

It is realistic to think that more materials from the past - originally overlooked for their potential in gas separations because not characterised for their adsorption properties - can be found that offer attractive performance for one or more separation processes using such a "low throughput" approach. The enterprise of dusting off "old" materials is therefore to be encouraged.

6.8 Elucidating adsorption mechanisms: from understanding to design

An important difference between MOFs and other solid sorbents is that MOFs display a range of unique adsorption mechanisms, not encountered in any other class of sorbents. Besides the fundamental scientific interest that the observation of a new phenomenon can arouse, there are cases where exotic adsorption behaviour can lead to significant enhancements in gas separation performance. It becomes crucial to investigate and understand such mechanisms in detail, if we want to take full advantage of them and design improved MOF sorbents based on the same working principle.

One of the most successful examples seen recently is represented by so-called amine-appended MOFs for CO_2 capture, first reported in 2012 (Figure 19a).[186] These sorbents are based on [M_2(dobpdc)] (M = Mg^{II}, Zn^{II}, Ni^{II}, Mn^{II}, Co^{II}), an isoreticular analogue of the prototypical MOF-74 with larger channel size. By grafting *N*,*N*'-dimethylethylenediamine (mmen) on the open metal sites exposed on the pore surface, the goal was to use the MOF as a simple support for aliphatic amines, akin to a silica matrix. However, it was found that CO_2 adsorption proceeded with an unusual step-shaped isotherm (Figure 19b). The adsorption mechanism was later elucidated by combination of experimental methods (i.e. X-ray diffraction, infrared spectroscopy, solid-state nuclear magnetic resonance, X-ray absorption spectroscopy) and quantum mechanical calculations.[181] It was revealed that CO_2 is not bound by the amine group exposed inside the channel, but by the amine coordinated to the metal atom. This results in the formation of a new metal-carbamate bond, accompanied by proton transfer to the uncoordinated amine group of a neighbouring mmen unit along the channel direction. This event leads to cooperative formation of ammonium-carbamate pairs stabilized by hydrogen bonding, explaining the observed step-shaped isotherm (Figure 19c). The CO_2 pressure at which this cooperative behaviour is triggered changes for different metals, as a result of the different strength of the amine-metal bond. Notably, the Mg-based isomer can capture CO_2 directly from the air.[186] Since the mechanism was first described, the same MOF matrix has been modified with a wide range of aliphatic diamines,[187,378,379] polyamines[380] and aminoalcohols,[381] thus giving rise to a large family of CO_2 sorbents based on the same working principle. This cooperative mechanism was also observed with CS_2 as the adsorbate.[382] As an additional point of interest concerning this mechanism, it was recently predicted by molecular dynamics simulations that adsorption of CO_2 in these sorbents can lead to an increase in thermal conductivity.[383] Given their potential for effective CO_2 capture from both concentrated and diluted sources, these MOFs have also raised the interest of engineers and have been the object of process simulation studies[44,49] and techno-economic analysis[384] to further assess their suitability as sorbents in an industrial setting.

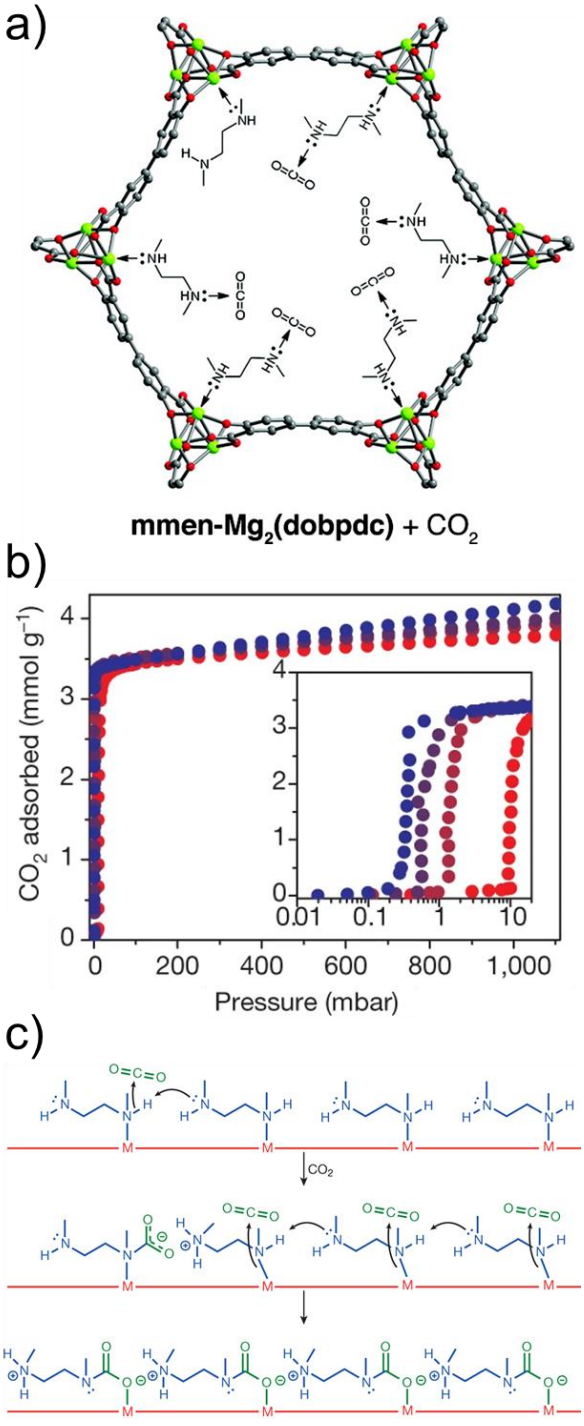

Figure 19. Crystal structure of mmen-Mg_2(dobpdc) (a), step-shaped CO_2 adsorption isotherms (b) and proposed cooperative CO_2 adsorption mechanism (c). Reprinted (adapted) with permission from McDonald et al. "Capture of Carbon Dioxide from Air and Flue Gas in the Alkylamine-Appended Metal–Organic Framework mmen-Mg_2(dobpdc)" J. Am. Chem. Soc. 2012, 134, 16, 7056–7065. Copyright 2012 American Chemical Society. Reprinted by permission from

Springer Nature: Nature 519, 303–308 (2015) "Cooperative insertion of CO_2 in diamine-appended metal-organic frameworks", Thomas M. McDonald et al. Copyright (2015).

The availability of open metal sites has been proven crucial to enable the adsorption of poorly interacting species, such as N_2 and O_2, taking advantage of unusual adsorption mechanisms. $[Cr_3(btc)_2]$[385] and MOF-74(Fe)[386] are rare examples of sorbents able to selectively bind O_2 over N_2. In both cases, a side-on interaction that involves both O atoms of the O_2 molecule and the open metal sites was observed by combining neutron diffraction, IR spectroscopy, X-ray absorption spectroscopy, UV-Vis-nIR spectroscopy and (in the case of the Fe-based MOF) Mössbauer spectroscopy. In $[Cr_3(btc)_2]$ adsorption of O_2 occurs with charge transfer between the metal and the adsorbate but does not involve a proper redox process. In MOF-74(Fe), instead, the Fe^{II} centres undergo partial oxidation at low temperature (< 222 K) and are completely oxidised at high temperature (> 222 K), making the process irreversible in the latter case. Late transition metals, such as Co, Ni and Zn, do not display the same affinity for O_2, due to the lack of available d-orbitals to accept electrons from the O atoms.[386] More recent examples of peculiar adsorption mechanisms involving specific binding of weakly interacting species with open metal sites are represented by the π backbonding interaction engaged by MIL-100(Cr)[387] and $[V_2Cl_{2.8}(btdd)]$[388] with N_2 and olefins. This sort of interaction is commonly seen in biologic systems and organometallic complexes[389] and allows to bind N_2 with very high heats of adsorption (up to 55 kJ mol^{-1} in $[V_2Cl_{2.8}(btdd)]$) and in a selective manner over O_2 and CH_4. In this case, there is still no recognised potential of any of the mentioned MOFs for real life separations, either because of reversibility issues (O_2 adsorption on $[Cr_3(btc)_2]$[385] and MOF-74(Fe)[386]) or because of the very recent appearance in the literature (N_2 adsorption on MIL-100(Cr)[387] and $[V_2Cl_{2.8}(btdd)]$[388]). However, these examples might serve as inspiration for new materials taking advantage of the same adsorption mechanism to selectively bind certain elusive species and enable challenging gas separations.

7. Outlook

The foregoing discussion provides a broad overview of the various levels of challenge that the development of MOF-based gas separation processes poses to chemists, material scientists and engineers. The task is a multifaceted one and, as such, it demands a holistic approach to be successfully accomplished. It is imperative to develop a cross-disciplinary partnership that can address the bottlenecks that are currently hampering progress. In the following, we provide a personal view of the main aspects that deserve attention in the immediate future.

With recent efforts in that direction, it is important to continue to lower barriers between disciplines, i.e. engineering vs chemistry/material science or computational vs experimental. Indeed, the input of a community is needed by the other and *vice versa*, as we have highlighted above. Hence, while a common language is probably utopian, one should aim to make the

messaging of a study accessible to the relevant communities and when appropriate to provide user-friendly tools and codes.

Focusing on computational work – at the molecular- and process-level – we note the following challenges. First, the number of MOF structures, process design variables and cycle types can render screening and optimisation studies very time-consuming. In that regard, the emergence of machine-learning studies could be a way forward. Second, any model requires experimental validation. Such validation, whether at the material characterisation/testing level (e.g. thermal and kinetic properties) or at the pilot-scale testing level, is sometimes limited by the availability of techniques and set-ups to assess such features. There is a need to continue generating sufficient and high-quality experimental data across all scales of the sorbent evaluation route and, for this to be possible, dedicated set-ups or commercial ones must be available. Finally, the ability to depict the complete sorption behaviour of MOFs remains difficult – for instance, accounting for the role of unsaturated metal sites is often done on an *ad hoc* basis – and efforts in this area must continue.

From an experimental point of view, we also highlight a number of possible future research directions. While much has been done experimentally to synthesise, characterise and test MOFs, more must be done to not only fill in gaps in data but also to appropriately report data. Having a complete profile of a MOF structure, properties and sorption behaviour remains a goal. Aiming for the generation of FAIR (findability, accessibility, interoperability, and reusability) data is a way forward. High-throughput studies, along with the use of repositories for MOFs properties, could support such endeavour. As hinted earlier, some MOF properties remain poorly investigated and/or understood (e.g. kinetics, multicomponent sorption behaviour, flexibility, thermal properties) and should become the focus of future efforts that, in some cases, could be supported with the development of commercial units to assess such properties. Finally, despite the many studies on MOFs, one could argue that only a small number of possible structures have been investigated, thereby limiting the reach of these materials. Enlarging the design space appears to be key and could be achieved in part by exploring new linkers, understanding better the self-assembly process and exploiting high-throughput synthesis platforms.

ACKNOWLEDGEMENT

C.P. is grateful to the EPSRC for providing the funding to undertake this research via the UK Carbon Capture and Storage Research Centre (UKCCSRC, grant EP/P026214/1). C.P. thanks Dr David Danaci (Imperial College London) for fruitful discussions related to adsorption-based process modelling.

Conflicts of interest

There are no conflicts of interest to declare.

References

1 C. J. King, in *Ullmann's Encyclopedia of Industrial Chemistry*, Wiley, 2000.
2 F. G. Kerry, *Industrial gas handbook - Gas separation and purification*, CRC Press, 2007.
3 D. S. Sholl and R. P. Lively, *Nature*, 2016, **532**, 435–437.
4 R. T. Yang, *Gas Separation by Adsorption Processes*, Elsevier, 1987.
5 P. Pullumbi, F. Brandani and S. Brandani, *Curr. Opin. Chem. Eng.*, 2019, **24**, 131–142.
6 W. J. Koros and G. K. Fleming, *J. Membr. Sci.*, 1993, **83**, 1–80.
7 M. Armstrong, B. Shan and B. Mu, in *Gas Adsorption in Metal-Organic Frameworks - Fundamentals and Applications*, CRC Press, 2019, pp. 83–108.
8 H. A. Patel, J. Byun and C. T. Yavuz, *ChemSusChem*, 2017, **10**, 1303–1317.
9 A. Alonso, J. Moral-Vico, A. Abo Markeb, M. Busquets-Fité, D. Komilis, V. Puntes, A. Sánchez and X. Font, *Sci. Total Environ.*, 2017, **595**, 51–62.
10 Y. Wu and B. M. Weckhuysen, *Angew. Chem. Int. Ed.*, 2021, anie.202104318.
11 D.-D. Zhou, X.-W. Zhang, Z.-W. Mo, Y.-Z. Xu, X.-Y. Tian, Y. Li, X.-M. Chen and J.-P. Zhang, *EnergyChem*, 2019, **1**, 100016.
12 M. W. Ackley, S. U. Rege and H. Saxena, *ZEOLITE 02 Proc. 6th Int. Conf. Occur. Prop. Util. Nat. Zeolites*, 2003, **61**, 25–42.
13 N. K. Jensen, T. E. Rufford, G. Watson, D. K. Zhang, K. I. Chan and E. F. May, *J. Chem. Eng. Data*, 2012, **57**, 106–113.
14 K. C. Kemp, J. G. Min, H. J. Choi and S. B. Hong, in *New Developments in Adsorption/Separation of Small Molecules by Zeolites*, eds. S. Valencia and F. Rey, Springer International Publishing, Cham, 2020, pp. 1–30.
15 D. Bonenfant, M. Kharoune, P. Niquette, M. Mimeault and R. Hausler, *Sci. Technol. Adv. Mater.*, 2008, **9**, 013007.
16 A. Janda and A. T. Bell, *J. Am. Chem. Soc.*, 2013, **135**, 19193–19207.
17 C.-T. Yang, A. Janda, A. T. Bell and L.-C. Lin, *J. Phys. Chem. C*, 2018, **122**, 9397–9410.
18 IZA structure database, http://www.iza-structure.org/databases/.
19 S. Sircar, T. C. Golden and M. B. Rao, *Carbon*, 1996, **34**, 1–12.
20 S. J. Allen, L. Whitten and G. Mckay, *Dev. Chem. Eng. Miner. Process.*, 1998, **6**, 231–261.
21 M. M. Maroto-Valer, Z. Tang and Y. Zhang, *Carbon Dioxide Capture Sequestration*, 2005, **86**, 1487–1502.
22 C. A. Grande, S. Cavenati, F. A. Da Silva and A. E. Rodrigues, *Ind. Eng. Chem. Res.*, 2005, **44**, 7218–7227.
23 V. Presser, J. McDonough, S.-H. Yeon and Y. Gogotsi, *Energy Env. Sci*, 2011, **4**, 3059–3066.
24 R. L. S. Canevesi, K. A. Andreassen, E. A. da Silva, C. E. Borba and C. A. Grande, *Ind. Eng. Chem. Res.*, 2018, **57**, 8057–8067.
25 S. Khodabakhshi, M. Taddei, J. A. Rudd, M. J. McPherson, Y. Niu, R. E. Palmer, A. R. Barron and E. Andreoli, *Carbon*, 2021, **173**, 989–1002.
26 J. P. Paraknowitsch and A. Thomas, *Energy Env. Sci*, 2013, **6**, 2839–2855.
27 B. Ashourirad, P. Arab, T. Islamoglu, K. A. Cychosz, M. Thommes and H. M. El-Kaderi, *J Mater Chem A*, 2016, **4**, 14693–14702.

28 B. Hu, K. Wang, L. Wu, S.-H. Yu, M. Antonietti and M.-M. Titirici, *Adv. Mater.*, 2010, **22**, 813–828.
29 T. J. Bandosz, *Activated Carbon Surfaces in Environmental Remediation*, Elsevier, 2006.
30 L. Öhrström and F. M. A. Noa, *Metal-Organic Frameworks*, American Chemical Society, 2021.
31 O. M. Yaghi, M. J. Kalmutzki and C. S. Diercks, *Introduction to Reticular Chemistry: Metal-Organic Frameworks and Covalent Organic Frameworks*, Wiley, 1st edn., 2019.
32 G. Férey, *Chem Soc Rev*, 2008, **37**, 191–214.
33 M. L. Foo, R. Matsuda and S. Kitagawa, *Chem. Mater.*, 2014, **26**, 310–322.
34 R. Freund, S. Canossa, S. M. Cohen, W. Yan, H. Deng, V. Guillerm, M. Eddaoudi, D. G. Madden, D. Fairen-Jimenez, H. Lyu, L. K. Macreadie, Z. Ji, Y. Zhang, B. Wang, F. Haase, C. Wöll, O. Zaremba, J. Andreo, S. Wuttke and C. S. Diercks, *Angew. Chem. Int. Ed.*, , DOI:10.1002/anie.202101644.
35 J.-R. Li, R. J. Kuppler and H.-C. Zhou, *Chem Soc Rev*, 2009, **38**, 1477–1504.
36 J. Yu, L.-H. Xie, J.-R. Li, Y. Ma, J. M. Seminario and P. B. Balbuena, *Chem. Rev.*, 2017, **117**, 9674–9754.
37 L. Yang, S. Qian, X. Wang, X. Cui, B. Chen and H. Xing, *Chem. Soc. Rev.*, 2020, **49**, 5359–5406.
38 R.-B. Lin, S. Xiang, H. Xing, W. Zhou and B. Chen, *Coord. Chem. Rev.*, 2019, 17.
39 S. Mukherjee, D. Sensharma, K.-J. Chen and M. J. Zaworotko, *Chem. Commun.*, 2020, **56**, 10419–10441.
40 C. Petit, *Nanotechnol. Sep. Eng.*, 2018, **20**, 132–142.
41 K. Adil, Y. Belmabkhout, R. S. Pillai, A. Cadiau, P. M. Bhatt, A. H. Assen, G. Maurin and M. Eddaoudi, *Chem. Soc. Rev.*, 2017, **46**, 3402–3430.
42 J. Liu, P. K. Thallapally, B. P. McGrail, D. R. Brown and J. Liu, *Chem. Soc. Rev.*, 2012, **41**, 2308–2322.
43 A.-M. Banu, D. Friedrich, S. Brandani and T. Düren, *Ind. Eng. Chem. Res.*, 2013, **52**, 9946–9957.
44 M. Hefti, L. Joss, Z. Bjelobrk and M. Mazzotti, *Faraday Discuss.*, 2016, **192**, 153–179.
45 R. Krishna, *RSC Adv.*, 2017, **7**, 35724–35737.
46 R. Krishna, *Sep. Purif. Technol.*, 2018, **194**, 281–300.
47 A. H. Farmahini, S. Krishnamurthy, D. Friedrich, S. Brandani and L. Sarkisov, *Ind. Eng. Chem. Res.*, 2018, **57**, 15491–15511.
48 A. K. Rajagopalan and A. Rajendran, *Int. J. Greenh. Gas Control*, 2018, **78**, 437–447.
49 K. N. Pai, J. D. Baboolal, D. A. Sharp and A. Rajendran, *Sep. Purif. Technol.*, 2019, **211**, 540–550.
50 D. Danaci, M. Bui, N. Mac Dowell and C. Petit, *Mol. Syst. Des. Eng.*, 2020, **5**, 212–231.
51 T. D. Burns, K. N. Pai, S. G. Subraveti, S. P. Collins, M. Krykunov, A. Rajendran and T. K. Woo, *Environ. Sci. Technol.*, 2020, **54**, 4536–4544.
52 A. H. Farmahini, S. Krishnamurthy, D. Friedrich, S. Brandani and L. Sarkisov, *arXiv:2009.12289*, 2020.
53 A. H. Farmahini, D. Friedrich, S. Brandani and L. Sarkisov, *Energy Environ. Sci.*, 2020, **13**, 1018–1037.

54 D. Yancy-Caballero, K. T. Leperi, B. J. Bucior, R. K. Richardson, T. Islamoglu, O. K. Farha, F. You and R. Q. Snurr, *Mol. Syst. Des. Eng.*, 2020, **5**, 1205–1218.
55 M. Asgari, A. Streb, M. van der Spek, W. Queen and M. Mazzotti, *Chem. Eng. J.*, 2021, **414**, 128778.
56 M. Khurana and S. Farooq, *Ind. Eng. Chem. Res.*, 2016, **55**, 2447–2460.
57 B. J. Maring and P. A. Webley, *Int. J. Greenh. Gas Control*, 2013, **15**, 16–31.
58 M. Khurana and S. Farooq, *AIChE J.*, 2019, **65**, 184–195.
59 Y. Wang and D. Zhao, *Cryst Growth Des*, 2017, 18.
60 H. Kim, S. Yang, S. R. Rao, S. Narayanan, E. A. Kapustin, H. Furukawa, A. S. Umans, O. M. Yaghi and E. N. Wang, *Science*, 2017, **356**, 430.
61 A. J. Rieth, S. Yang, E. N. Wang and M. Dincă, *ACS Cent. Sci.*, 2017, **3**, 668–672.
62 F. Fathieh, M. J. Kalmutzki, E. A. Kapustin, P. J. Waller, J. Yang and O. M. Yaghi, *Sci. Adv.*, 2018, **4**, eaat3198.
63 N. Hanikel, M. S. Prévot, F. Fathieh, E. A. Kapustin, H. Lyu, H. Wang, N. J. Diercks, T. G. Glover and O. M. Yaghi, *ACS Cent. Sci.*, 2019, **5**, 1699–1706.
64 S. M. Towsif Abtab, D. Alezi, P. M. Bhatt, A. Shkurenko, Y. Belmabkhout, H. Aggarwal, Ł. J. Weseliński, N. Alsadun, U. Samin, M. N. Hedhili and M. Eddaoudi, *Chem*, 2018, **4**, 94–105.
65 M. E. Boot-Handford, J. C. Abanades, E. J. Anthony, M. J. Blunt, S. Brandani, N. Mac Dowell, J. R. Fernández, M.-C. Ferrari, R. Gross, J. P. Hallett, R. S. Haszeldine, P. Heptonstall, A. Lyngfelt, Z. Makuch, E. Mangano, R. T. J. Porter, M. Pourkashanian, G. T. Rochelle, N. Shah, J. G. Yao and P. S. Fennell, *Energy Environ. Sci.*, 2014, **7**, 130–189.
66 M. Bui, C. S. Adjiman, A. Bardow, E. J. Anthony, A. Boston, S. Brown, P. S. Fennell, S. Fuss, A. Galindo, L. A. Hackett, J. P. Hallett, H. J. Herzog, G. Jackson, J. Kemper, S. Krevor, G. C. Maitland, M. Matuszewski, I. S. Metcalfe, C. Petit, G. Puxty, J. Reimer, D. M. Reiner, E. S. Rubin, S. A. Scott, N. Shah, B. Smit, J. P. M. Trusler, P. Webley, J. Wilcox and N. Mac Dowell, *Energy Environ. Sci.*, 2018, **11**, 1062–1176.
67 K. Sumida, D. L. Rogow, J. A. Mason, T. M. McDonald, E. D. Bloch, Z. R. Herm, T.-H. Bae and J. R. Long, *Chem. Rev.*, 2012, **112**, 724–781.
68 A. F. Ismail, K. C. Khulbe and T. Matsuura, in *Gas Separation Membranes: Polymeric and Inorganic*, eds. A. F. Ismail, K. Chandra Khulbe and T. Matsuura, Springer International Publishing, Cham, 2015, pp. 11–35.
69 A. D. Buckingham, R. L. Disch and D. A. Dunmur, *J. Am. Chem. Soc.*, 1968, **90**, 3104–3107.
70 G. T. Rochelle, *Science*, 2009, **325**, 1652–1654.
58 O. Ghaffari-Nik, L. Mariac, A. Liu, B. Henkel, S. Marx and P. Hovington, Rapid Cycle Temperature Swing Adsorption Process Using Solid Structured Sorbent for CO2 capture from Cement Flue Gas, 15th International Conference on Greenhouse Gas Control Technologies, GHGT-15, 2021.
59 US9782745B2, Metal organic framework, production and use thereof.
60 WO2019204934A1, Synthesis of zinc mof materials.
74 E. S. Sanz-Pérez, C. R. Murdock, S. A. Didas and C. W. Jones, *Chem. Rev.*, 2016, **116**, 11840–11876.
75 J. Wilcox, P. C. Psarras and S. Liguori, *Environ. Res. Lett.*, 2017, **12**, 065001.
76 N. McQueen, K. V. Gomes, C. McCormick, K. Blumanthal, M. Pisciotta and J. Wilcox, *Prog. Energy*, 2021, **3**, 032001.

77 J. D. Holladay, J. Hu, D. L. King and Y. Wang, *Hydrog. Prod. - Sel. Pap. Hydrog. Prod. Symp. Am. Chem. Soc. 234th Natl. Meet. Expo. August 19-23 2007 Boston MA USA*, 2009, **139**, 244–260.
78 S. Sircar and T. C. Golden, *Sep. Sci. Technol.*, 2000, **35**, 667–687.
79 I. Angelidaki, L. Xie, G. Luo, Y. Zhang, H. Oechsner, A. Lemmer, R. Munoz and P. G. Kougias, in *Biofuels: Alternative Feedstocks and Conversion Processes for the Production of Liquid and Gaseous Biofuels*, Elsevier, 2019, pp. 817–843.
80 T. Remy, E. Gobechiya, D. Danaci, S. A. Peter, P. Xiao, L. Van Tendeloo, S. Couck, J. Shang, C. E. A. Kirschhock, R. K. Singh, J. A. Martens, G. V. Baron, P. A. Webley and J. F. M. Denayer, *RSC Adv*, 2014, **4**, 62511–62524.
81 H. Demir, C. J. Cramer and J. I. Siepmann, *Mol. Syst. Des. Eng.*, 2019, **4**, 1125–1135.
82 C. A. Grande and A. E. Rodrigues, *Ind. Eng. Chem. Res.*, 2007, **46**, 4595–4605.
83 A. J. Kidnay and W. R. Parrish, *Fundamentals of Natural Gas Processing*, CRC Press, 2006.
84 G. Hammer, T. Lübcke, R. Kettner, M. R. Pillarella, H. Recknagel, A. Commichau, H.-J. Neumann and B. Paczynska-Lahme, in *Ullmann's Encyclopedia of Industrial Chemistry*, Wiley, 2006.
85 M. J. Kirschner, A. Alekseev, S. Dowy, M. Grahl, L. Jansson, P. Keil, G. Lauermann, M. Meilinger, W. Schmehl, H. Weckler and C. Windmeier, in *Ullmann's Encyclopedia of Industrial Chemistry*, Wiley, 2017, pp. 1–32.
86 N. Böcker, M. Grahl, A. Tota, P. Häussinger, P. Leitgeb and B. Schmücker, in *Ullmann's Encyclopedia of Industrial Chemistry*, Wiley, 2013, pp. 1–27.
87 S. U. Rege and R. T. Yang, *Ind. Eng. Chem. Res.*, 1997, **36**, 5358–5365.
88 P. Pässler, W. Hefner, K. Buckl, H. Meinass, A. Meiswinkel, H.-J. Wernicke, G. Ebersberg, R. Müller, J. Bässler, H. Behringer and D. Mayer, in *Ullmann's Encyclopedia of Industrial Chemistry*, Wiley, 2011, pp. 277–326.
89 K.-J. Chen, H. S. Scott, D. G. Madden, T. Pham, A. Kumar, A. Bajpai, M. Lusi, K. A. Forrest, B. Space, J. J. Perry and M. J. Zaworotko, *Chem*, 2016, **1**, 753–765.
90 X.-P. Fu, Y.-L. Wang and Q.-Y. Liu, *Dalton Trans.*, 2020, 10.
91 A. Nemati Vesali Azar and S. Keskin, *Front. Chem.*, 2018, **6**, 36.
92 H. Zimmermann and R. Walzl, in *Ullmann's Encyclopedia of Industrial Chemistry*, Wiley, 2009.
93 H. Zimmermann, in *Ullmann's Encyclopedia of Industrial Chemistry*, Wiley, 2013, pp. 00–00.
94 R. Lyndon, W. You, Y. Ma, J. Bacsa, Y. Gong, E. E. Stangland, K. S. Walton, D. S. Sholl and R. P. Lively, *Chem. Mater.*, 2020, **32**, 3715–3722.
95 R.-B. Lin, L. Li, H.-L. Zhou, H. Wu, C. He, S. Li, R. Krishna, J. Li, W. Zhou and B. Chen, *Nat. Mater.*, 2018, **17**, 1128–1133.
96 C. Y. Lee, Y.-S. Bae, N. C. Jeong, O. K. Farha, A. A. Sarjeant, C. L. Stern, P. Nickias, R. Q. Snurr, J. T. Hupp and S. T. Nguyen, *J. Am. Chem. Soc.*, 2011, **133**, 5228–5231.
97 L. Li, R.-B. Lin, X. Wang, W. Zhou, L. Jia, J. Li and B. Chen, *Chem. Eng. J.*, 2018, **354**, 977–982.
98 O. T. Qazvini and S. G. Telfer, *J. Mater. Chem. A*, 2020, **8**, 12028–12034.
99 R. B. Eldridge, *Ind. Eng. Chem. Res.*, 1993, **32**, 2208–2212.
100 D. Danaci, P. A. Webley and C. Petit, *Front. Chem. Eng.*, 2021, **2**, 602430.

101 A. K. Rajagopalan, A. M. Avila and A. Rajendran, *Int. J. Greenh. Gas Control*, 2016, **46**, 76–85.
102 J. M. Huck, L.-C. Lin, A. H. Berger, M. N. Shahrak, R. L. Martin, A. S. Bhown, M. Haranczyk, K. Reuter and B. Smit, *Energy Env. Sci*, 2014, **7**, 4132–4146.
103 B. Mu and K. S. Walton, *J. Phys. Chem. C*, 2011, **115**, 22748–22754.
104 F. A. Kloutse, R. Zacharia, D. Cossement and R. Chahine, *Microporous Mesoporous Mater.*, 2015, **217**, 1–5.
105 S. Cui, A. Marandi, G. Lebourleux, M. Thimon, M. Bourdon, C. Chen, M. I. Severino, V. Steggles, F. Nouar and C. Serre, *Appl. Therm. Eng.*, 2019, **161**, 114135.
106 Y. Luo, W. Cui, Y. Zou, H. Chu, F. Xu and L. Sun, *J. Therm. Anal. Calorim.*, 2020, **142**, 891–898.
107 H. Babaei and C. E. Wilmer, *Phys. Rev. Lett.*, 2016, **116**, 025902.
108 H. Babaei, A. J. H. McGaughey and C. E. Wilmer, *Chem. Sci.*, 2017, **8**, 583–589.
109 K. B. Sezginel, P. A. Asinger, H. Babaei and C. E. Wilmer, *Chem. Mater.*, 2018, **30**, 2281–2286.
110 K. B. Sezginel, S. Lee, H. Babaei and C. E. Wilmer, *J. Phys. Chem. C*, 2020, **124**, 18604–18608.
111 P. Ying, J. Zhang, X. Zhang and Z. Zhong, *J. Phys. Chem. C*, 2020, **124**, 6274–6283.
112 A. Lamaire, J. Wieme, A. E. J. Hoffman and V. Van Speybroeck, *Faraday Discuss.*, 2021, **225**, 301–323.
113 J. Wieme, S. Vandenbrande, A. Lamaire, V. Kapil, L. Vanduyfhuys and V. Van Speybroeck, *ACS Appl. Mater. Interfaces*, 2019, **11**, 38697–38707.
114 A. Chakraborty, B. B. Saha, S. Koyama and K. C. Ng, *Appl. Phys. Lett.*, 2007, **90**, 171902.
115 K. A. Rahman, W. S. Loh and K. C. Ng, *Procedia Eng.*, 2013, **56**, 118–125.
116 V. Schwamberger and F. P. Schmidt, *Ind. Eng. Chem. Res.*, 2013, **52**, 16958–16965.
117 H. Babaei, M. E. DeCoster, M. Jeong, Z. M. Hassan, T. Islamoglu, H. Baumgart, A. J. H. McGaughey, E. Redel, O. K. Farha, P. E. Hopkins, J. A. Malen and C. E. Wilmer, *Nat. Commun.*, 2020, **11**, 4010.
118 D. DeSantis, J. A. Mason, B. D. James, C. Houchins, J. R. Long and M. Veenstra, *Energy Fuels*, 2017, **31**, 2024–2032.
119 G. Schukraft and C. Petit, in *Sustainable Nanoscale Engineering*, eds. G. Szekely and A. Livingston, Elsevier, 2020, pp. 139–162.
120 K. N. Pai, V. Prasad and A. Rajendran, *ACS Sustain. Chem. Eng.*, 2021, **9**, 3838–3849.
121 K. T. Leperi, Y. G. Chung, F. You and R. Q. Snurr, *ACS Sustain. Chem. Eng.*, 2019, **7**, 11529–11539.
122 V. Subramanian Balashankar and A. Rajendran, *ACS Sustain. Chem. Eng.*, 2019, **7**, 17747–17755.
123 D. Dubbeldam, S. Calero, D. E. Ellis and R. Q. Snurr, *Mol. Simul.*, 2016, **42**, 81–101.
124 P. Z. Moghadam, A. Li, S. B. Wiggin, A. Tao, A. G. P. Maloney, P. A. Wood, S. C. Ward and D. Fairen-Jimenez, *Chem. Mater.*, 2017, **29**, 2618–2625.
125 CSD MOF Subset, https://sites.google.com/view/csdmofsubset/home.
126 Y. G. Chung, J. Camp, M. Haranczyk, B. J. Sikora, W. Bury, V. Krungleviciute, T. Yildirim, O. K. Farha, D. S. Sholl and R. Q. Snurr, *Chem. Mater.*, 2014, **26**, 6185–6192.
127 CoRE MOF Database, https://cmcp-group.github.io/CoRE-MOFs/.

128 R. Haghpanah, R. Nilam, A. Rajendran, S. Farooq and I. A. Karimi, *AIChE J.*, 2013, **59**, 4735–4748.
129 L. Joss, M. Gazzani and M. Mazzotti, *Chem. Eng. Sci.*, 2017, **158**, 381–394.
130 S. U. Rege and R. T. Yang, *Sep. Sci. Technol.*, 2001, **36**, 3355–3365.
131 Y.-S. Bae and R. Q. Snurr, *Angew Chem Int Ed*, 2011, 11.
132 A. D. Wiersum, J.-S. Chang, C. Serre and P. L. Llewellyn, *Langmuir*, 2013, **29**, 3301–3309.
133 J. Park, H. O. Rubiera Landa, Y. Kawajiri, M. J. Realff, R. P. Lively and D. S. Sholl, *Ind. Eng. Chem. Res.*, 2020, **59**, 7097–7108.
134 The NIST Registry of Adsorbent Materials, https://adsorption.nist.gov/matdb/index.php#home.
135 NIST Isotherm Database, https://github.com/NIST-ISODB.
136 P. Iacomi and P. L. Llewellyn, *ChemRxiv*, 2019.
137 J. D. Evans, V. Bon, I. Senkovska and S. Kaskel, *Langmuir*, 2021, **37**, 4222–4226.
138 S. R. Hall and N. Spadaccini, *J. Chem. Inf. Comput. Sci.*, 1994, **34**, 505–508.
139 M. Rahimi, S. M. Moosavi, B. Smit and T. A. Hatton, *Cell Rep. Phys. Sci.*, 2021, **2**, 100396.
140 S. G. Subraveti, Z. Li, V. Prasad and A. Rajendran, *Ind. Eng. Chem. Res.*, 2019, **58**, 20412–20422.
141 K. N. Pai, V. Prasad and A. Rajendran, *Ind. Eng. Chem. Res.*, 2020, **59**, 16730–16740.
142 K. N. Pai, V. Prasad and A. Rajendran, *Sep. Purif. Technol.*, 2020, **241**, 116651.
143 R. Anderson, A. Biong and D. A. Gómez-Gualdrón, *J. Chem. Theory Comput.*, 2020, **16**, 1271–1283.
144 X. Zhu, D. C. W. Tsang, L. Wang, Z. Su, D. Hou, L. Li and J. Shang, *J. Clean. Prod.*, 2020, **273**, 122915.
145 I. G. Clayson, D. Hewitt, M. Hutereau, T. Pope and B. Slater, *Adv Mater*, 2020, 47.
146 J. A. Mason, T. M. McDonald, T.-H. Bae, J. E. Bachman, K. Sumida, J. J. Dutton, S. S. Kaye and J. R. Long, *J. Am. Chem. Soc.*, 2015, **137**, 4787–4803.
147 http://aam.ceb.cam.ac.uk/mofexplorer.html, http://aam.ceb.cam.ac.uk/mofexplorer.html.
148 S. Krishnamurthy, V. R. Rao, S. Guntuka, P. Sharratt, R. Haghpanah, A. Rajendran, M. Amanullah, I. A. Karimi and S. Farooq, *AIChE J.*, 2014, **60**, 1830–1842.
149 S. Brandani and E. Mangano, *Adsorption*, 2021, **27**, 319–351.
150 A. C. Forse, C. Merlet, C. P. Grey and J. M. Griffin, *Prog. Nucl. Magn. Reson. Spectrosc.*, 2021, **124–125**, 57–84.
151 H. G. Karge and J. Kärger, in *Adsorption and Diffusion*, eds. H. G. Karge and J. Weitkamp, Springer Berlin Heidelberg, Berlin, Heidelberg, 2008, pp. 135–206.
152 D. M. Ruthven, J. Kärger, S. Brandani and E. Mangano, *Adsorption*, , DOI:10.1007/s10450-020-00257-w.
153 J. Kärger and Y. Wang, in *Gas Adsorption in Metal-Organic Frameworks*, CRC Press, 2018, pp. 109–204.
154 J. Kärger and D. M. Ruthven, *New J. Chem.*, 2016, **40**, 4027–4048.
155 S. Lawson, X. Li, H. Thakkar, A. A. Rownaghi and F. Rezaei, *Chem. Rev.*, 2021, **121**, 6246–6291.
156 D. Danaci, P. A. Webley and C. Petit, *Front. Chem. Eng.*, 2021, **2**, 602430.

157 M. I. Severino, E. Gkaniatsou, F. Nouar, M. L. Pinto and C. Serre, *Faraday Discuss.*, , DOI:10.1039/D1FD00018G.
158 Z. Hu, Y. Wang, B. B. Shah and D. Zhao, *Adv. Sustain. Syst.*, 2019, **3**, 1800080.
159 A. Sturluson, M. T. Huynh, A. R. Kaija, C. Laird, S. Yoon, F. Hou, Z. Feng, C. E. Wilmer, Y. J. Colón, Y. G. Chung, D. W. Siderius and C. M. Simon, *Mol. Simul.*, 2019, **45**, 1082–1121.
160 D. P. Broom, in *Hydrogen Storage Materials: The Characterisation of Their Storage Properties*, ed. D. P. Broom, Springer London, London, 2011, pp. 117–139.
161 S. Sircar, H. Wu, J. Li and A. D. Lueking, *Langmuir*, 2011, **27**, 14169–14179.
162 C. Serre, F. Millange, C. Thouvenot, M. Noguès, G. Marsolier, D. Louër and G. Férey, *J. Am. Chem. Soc.*, 2002, **124**, 13519–13526.
163 S. Brunauer, P. H. Emmett and E. Teller, *J. Am. Chem. Soc.*, 1938, **60**, 309–319.
164 G. Horvath and K. Kawazoe, *J. Chem. Eng. Jpn.*, 1983, **16**, 470–475.
165 J. Rouquerol, P. Llewellyn and F. Rouquerol, in *Studies in Surface Science and Catalysis*, eds. P. L. Llewellyn, F. Rodriquez-Reinoso, J. Rouqerol and N. Seaton, Elsevier, 2007, vol. 160, pp. 49–56.
166 K. S. Walton and R. Q. Snurr, *J. Am. Chem. Soc.*, 2007, **129**, 8552–8556.
167 C. M. Lastoskie, in *Studies in Surface Science and Catalysis*, eds. K. K. Unger, G. Kreysa and J. P. Baselt, Elsevier, 2000, vol. 128, pp. 475–484.
168 C. Lastoskie, K. E. Gubbins and N. Quirke, *J. Phys. Chem.*, 1993, **97**, 4786–4796.
169 A. V. Neimark, Y. Lin, P. I. Ravikovitch and M. Thommes, *Carbon*, 2009, **47**, 1617–1628.
170 S. Dantas and A. V. Neimark, *ACS Appl. Mater. Interfaces*, 2020, **12**, 15595–15605.
171 D. W. Siderius, N. A. Mahynski and V. K. Shen, *Adsorption*, 2017, **23**, 593–602.
172 S. Mukherjee, S. Chen, A. A. Bezrukov, M. Mostrom, V. V. Terskikh, D. Franz, S. Wang, A. Kumar, M. Chen, B. Space, Y. Huang and M. J. Zaworotko, *Angew. Chem. Int. Ed.*, 2020, **59**, 16188–16194.
173 M. John Platers, R. Alan Howie and A. J. Roberts, *Chem. Commun.*, 1997, 893–894.
174 R. Vaidhyanathan, S. S. Iremonger, K. W. Dawson and G. K. H. Shimizu, *Chem. Commun.*, 2009, 5230–5232.
175 R. Vaidhyanathan, S. S. Iremonger, G. K. H. Shimizu, P. G. Boyd, S. Alavi and T. K. Woo, *Science*, 2010, **330**, 650.
176 J. I. Feldblyum, M. Liu, D. W. Gidley and A. J. Matzger, *J. Am. Chem. Soc.*, 2011, **133**, 18257–18263.
177 A. W. Thornton, K. E. Jelfs, K. Konstas, C. M. Doherty, A. J. Hill, A. K. Cheetham and T. D. Bennett, *Chem Commun*, 2016, **52**, 3750–3753.
178 N. S. Wilkins, A. Rajendran and S. Farooq, *Adsorption*, 2021, **27**, 397–422.
179 N. S. Wilkins and A. Rajendran, *Adsorption*, 2019, **25**, 115–133.
180 R. R. Vemula and S. Sircar, *AIChE J.*, 2017, **63**, 4066–4078.
181 T. M. McDonald, J. A. Mason, X. Kong, E. D. Bloch, D. Gygi, A. Dani, V. Crocellà, F. Giordanino, S. O. Odoh, W. S. Drisdell, B. Vlaisavljevich, A. L. Dzubak, R. Poloni, S. K. Schnell, N. Planas, K. Lee, T. Pascal, L. F. Wan, D. Prendergast, J. B. Neaton, B. Smit, J. B. Kortright, L. Gagliardi, S. Bordiga, J. A. Reimer and J. R. Long, *Nature*, 2015, **519**, 303–308.
182 C.-J. Yoo, S. J. Park and C. W. Jones, *Ind. Eng. Chem. Res.*, 2020, **59**, 7061–7071.
183 A. Koutsianos, A. R. Barron and E. Andreoli, *J. Phys. Chem. C*, 2017, **121**, 21772–21781.

184 S. J. Park, J. J. Lee, C. B. Hoyt, D. R. Kumar and C. W. Jones, *Adsorption*, 2020, **26**, 89–101.
185 A. Koutsianos, L. B. Hamdy, C.-J. Yoo, J. J. Lee, M. Taddei, J. M. Urban-Klaehn, J. Dryzek, C. W. Jones, A. R. Barron and E. Andreoli, *J. Mater. Chem. A*, 2021, **9**, 10827–10837.
186 T. M. McDonald, W. R. Lee, J. A. Mason, B. M. Wiers, C. S. Hong and J. R. Long, *J. Am. Chem. Soc.*, 2012, **134**, 7056–7065.
187 P. J. Milner, J. D. Martell, R. L. Siegelman, D. Gygi, S. C. Weston and J. R. Long, *Chem. Sci.*, 2018, **9**, 160–174.
188 M. Taddei, M. J. McPherson, A. Gougsa, J. Lam, J. Sewell and E. Andreoli, *Inorganics*, 2019, **7**, 9.
189 J. D. Martell, P. J. Milner, R. L. Siegelman and J. R. Long, *Chem. Sci.*, 2020, **11**, 6457–6471.
190 A. L. Myers and J. M. Prausnitz, *AIChE J.*, 1965, **11**, 121–127.
191 K. S. Walton and D. S. Sholl, *AIChE J.*, 2015, **61**, 2757–2762.
192 S. Lee, J. H. Lee and J. Kim, *Korean J. Chem. Eng.*, 2018, **35**, 214–221.
193 C. M. Simon, B. Smit and M. Haranczyk, *Comput. Phys. Commun.*, 2016, **200**, 364–380.
194 C.-W. Wu and S. Sircar, *Sep. Purif. Technol.*, 2016, **170**, 453–461.
195 X. Cai, F. Gharagheizi, L. W. Bingel, D. Shade, K. S. Walton and D. S. Sholl, *Ind. Eng. Chem. Res.*, 2021, **60**, 639–651.
196 A. Nuhnen and C. Janiak, *Dalton Trans.*, 2020, **49**, 10295–10307.
197 P. L. Llewellyn and G. Maurin, *Cryst. Organ. Porous Solids*, 2005, **8**, 283–302.
198 J. A. Dunne, R. Mariwala, M. Rao, S. Sircar, R. J. Gorte and A. L. Myers, *Langmuir*, 1996, **12**, 5888–5895.
199 M. E. Potter, S. H. Pang and C. W. Jones, *Langmuir*, 2017, **33**, 117–124.
200 K. S. Sánchez-Zambrano, E. Vilarrasa-García, D. A. S. Maia, M. Bastos-Neto, E. Rodríguez-Castellon and D. C. S. Azevedo, *Adsorption*, 2020, **26**, 165–175.
201 NIST Chemistry WebBook - Carbon Dioxide, https://webbook.nist.gov/cgi/cbook.cgi?ID=C124389&Mask=4.
202 M. Karimi, A. E. Rodrigues and J. A. C. Silva, *Chem. Eng. J.*, 2021, **425**, 130538.
203 Y. J. Colón and R. Q. Snurr, *Chem Soc Rev*, 2014, **43**, 5735–5749.
204 H. Daglar and S. Keskin, *Coord. Chem. Rev.*, 2020, **422**, 213470.
205 D. Wu, Q. Yang, C. Zhong, D. Liu, H. Huang, W. Zhang and G. Maurin, *Langmuir*, 2012, **28**, 12094–12099.
206 L.-C. Lin, A. H. Berger, R. L. Martin, J. Kim, J. A. Swisher, K. Jariwala, C. H. Rycroft, A. S. Bhown, M. W. Deem, M. Haranczyk and B. Smit, *Nat. Mater.*, 2012, **11**, 633–641.
207 E. Braun, A. F. Zurhelle, W. Thijssen, S. K. Schnell, L.-C. Lin, J. Kim, J. A. Thompson and B. Smit, *Mol. Syst. Des. Eng.*, 2016, **1**, 175–188.
208 A. Ö. Yazaydın, R. Q. Snurr, T.-H. Park, K. Koh, J. Liu, M. D. LeVan, A. I. Benin, P. Jakubczak, M. Lanuza, D. B. Galloway, J. J. Low and R. R. Willis, *J. Am. Chem. Soc.*, 2009, **131**, 18198–18199.
209 C. E. Wilmer, O. K. Farha, Y.-S. Bae, J. T. Hupp and R. Q. Snurr, *Energy Environ. Sci.*, 2012, **5**, 9849.

210 Y. G. Chung, D. A. Gómez-Gualdrón, P. Li, K. T. Leperi, P. Deria, H. Zhang, N. A. Vermeulen, J. F. Stoddart, F. You, J. T. Hupp, O. K. Farha and R. Q. Snurr, *Sci. Adv.*, 2016, **2**, e1600909.
211 S. Li, Y. G. Chung and R. Q. Snurr, *Langmuir*, 2016, **32**, 10368–10376.
212 M. Z. Aghaji, M. Fernandez, P. G. Boyd, T. D. Daff and T. K. Woo, *Eur. J. Inorg. Chem.*, 2016, **2016**, 4505–4511.
213 H. Dureckova, M. Krykunov, M. Z. Aghaji and T. K. Woo, *J. Phys. Chem. C*, 2019, **123**, 4133–4139.
214 J. Burner, L. Schwiedrzik, M. Krykunov, J. Luo, P. G. Boyd and T. K. Woo, *J. Phys. Chem. C*, 2020, **124**, 27996–28005.
215 R. Anderson, J. Rodgers, E. Argueta, A. Biong and D. A. Gómez-Gualdrón, *Chem. Mater.*, 2018, **30**, 6325–6337.
216 M. Fernandez and A. S. Barnard, *ACS Comb. Sci.*, 2016, **18**, 243–252.
217 C. Altintas, G. Avci, H. Daglar, A. Nemati Vesali Azar, S. Velioglu, I. Erucar and S. Keskin, *ACS Appl. Mater. Interfaces*, 2018, **10**, 17257–17268.
218 G. Avci, I. Erucar and S. Keskin, *ACS Appl. Mater. Interfaces*, 2020, **12**, 41567–41579.
219 S. Velioglu and S. Keskin, *Mater. Adv.*, 2020, **1**, 341–353.
220 Y. K. Ponraj and B. Borah, *J. Phys. Chem. C*, 2021, **125**, 1839–1854.
221 B. C. Yeo, D. Kim, H. Kim and S. S. Han, *J. Phys. Chem. C*, 2016, **120**, 24224–24230.
222 V. A. Solanki and B. Borah, *Mol. Simul.*, 2020, **46**, 1362–1372.
223 C. Gu, Z. Yu, J. Liu and D. S. Sholl, *ACS Appl. Mater. Interfaces*, 2021, **13**, 11039–11049.
224 B. J. Sikora, C. E. Wilmer, M. L. Greenfield and R. Q. Snurr, *Chem. Sci.*, 2012, **3**, 2217.
225 D. Banerjee, C. M. Simon, A. M. Plonka, R. K. Motkuri, J. Liu, X. Chen, B. Smit, J. B. Parise, M. Haranczyk and P. K. Thallapally, *Nat. Commun.*, 2016, **7**, ncomms11831.
226 T. Watanabe and D. S. Sholl, *Langmuir*, 2012, **28**, 14114–14128.
227 D. Ongari, L. Talirz and B. Smit, *ACS Cent. Sci.*, 2020, **6**, 1890–1900.
228 C. E. Wilmer, M. Leaf, C. Y. Lee, O. K. Farha, B. G. Hauser, J. T. Hupp and R. Q. Snurr, *Nat. Chem.*, 2012, **4**, 83–89.
229 Y. J. Colón, D. A. Gómez-Gualdrón and R. Q. Snurr, *Cryst. Growth Des.*, 2017, **17**, 5801–5810.
230 P. G. Boyd and T. K. Woo, *CrystEngComm*, 2016, **18**, 3777–3792.
231 P. Z. Moghadam, T. Islamoglu, S. Goswami, J. Exley, M. Fantham, C. F. Kaminski, R. Q. Snurr, O. K. Farha and D. Fairen-Jimenez, *Nat. Commun.*, 2018, **9**, 1378.
232 N. S. Bobbitt, J. Chen and R. Q. Snurr, *J. Phys. Chem. C*, 2016, **120**, 27328–27341.
233 S. Lee, B. Kim, H. Cho, H. Lee, S. Y. Lee, E. S. Cho and J. Kim, *ACS Appl. Mater. Interfaces*, 2021, **13**, 23647–23654.
234 A. Ahmed, S. Seth, J. Purewal, A. G. Wong-Foy, M. Veenstra, A. J. Matzger and D. J. Siegel, *Nat. Commun.*, 2019, **10**, 1568.
235 C. E. Wilmer and R. Q. Snurr, *Chem. Eng. J.*, 2011, **171**, 775–781.
236 E. Haldoupis, S. Nair and D. S. Sholl, *J. Am. Chem. Soc.*, 2012, **134**, 4313–4323.
237 C. Altintas and S. Keskin, *Mol. Syst. Des. Eng.*, 2020, **5**, 532–543.
238 P.-Q. Liao, H. Chen, D.-D. Zhou, S.-Y. Liu, C.-T. He, Z. Rui, H. Ji, J.-P. Zhang and X.-M. Chen, *Energy Env. Sci*, 2015, **8**, 1011–1016.

239 S. Xiang, X. Wu, J. Zhang, R. Fu, S. Hu and X. Zhang, *J. Am. Chem. Soc.*, 2005, **127**, 16352–16353.
240 S. Xiang, Y. He, Z. Zhang, H. Wu, W. Zhou, R. Krishna and B. Chen, *Nat. Commun.*, 2012, **3**, 954.
241 S. Nandi, P. De Luna, T. D. Daff, J. Rother, M. Liu, W. Buchanan, A. I. Hawari, T. K. Woo and R. Vaidhyanathan, *Sci. Adv.*, 2015, **1**, e1500421.
242 S. Nandi, S. Collins, D. Chakraborty, D. Banerjee, P. K. Thallapally, T. K. Woo and R. Vaidhyanathan, *J. Am. Chem. Soc.*, 2017, **139**, 1734–1737.
243 P. Nugent, Y. Belmabkhout, S. D. Burd, A. J. Cairns, R. Luebke, K. Forrest, T. Pham, S. Ma, B. Space, L. Wojtas, M. Eddaoudi and M. J. Zaworotko, *Nature*, 2013, **495**, 80–84.
244 O. M. Yaghi, *ACS Cent. Sci.*, 2019, **5**, 1295–1300.
245 M. Eddaoudi, J. Kim, N. Rosi, D. Vodak, J. Wachter, M. O'Keeffe and O. M. Yaghi, *Science*, 2002, **295**, 469.
246 H. Furukawa, K. E. Cordova, M. O'Keeffe and O. M. Yaghi, *Science*, 2013, **341**, 1230444.
247 I. Senkovska and S. Kaskel, *Chem Commun*, 2014, **50**, 7089–7098.
248 O. K. Farha, I. Eryazici, N. C. Jeong, B. G. Hauser, C. E. Wilmer, A. A. Sarjeant, R. Q. Snurr, S. T. Nguyen, A. Ö. Yazaydın and J. T. Hupp, *J. Am. Chem. Soc.*, 2012, **134**, 15016–15021.
249 M. F. de Lange, K. J. F. M. Verouden, T. J. H. Vlugt, J. Gascon and F. Kapteijn, *Chem. Rev.*, 2015, **115**, 12205–12250.
250 L. Wang, Y. Han, X. Feng, J. Zhou, P. Qi and B. Wang, *Chem. Appl. Met. Org. Framew.*, 2016, **307**, 361–381.
251 A. Bavykina, N. Kolobov, I. S. Khan, J. A. Bau, A. Ramirez and J. Gascon, *Chem. Rev.*, 2020, **120**, 8468–8535.
252 M. Oschatz and M. Antonietti, *Energy Environ. Sci.*, 2018, **11**, 57–70.
253 Y. Belmabkhout, V. Guillerm and M. Eddaoudi, *Chem. Eng. J.*, 2016, **296**, 386–397.
254 M. Ding, X. Cai and H.-L. Jiang, *Chem Sci*, 2019, **10**, 10209–10230.
255 N. C. Burtch, H. Jasuja and K. S. Walton, *Chem. Rev.*, 2014, **114**, 10575–10612.
256 S. Yuan, L. Feng, K. Wang, J. Pang, M. Bosch, C. Lollar, Y. Sun, J. Qin, X. Yang, P. Zhang, Q. Wang, L. Zou, Y. Zhang, L. Zhang, Y. Fang, J. Li and H.-C. Zhou, *Adv. Mater.*, 2018, **30**, 1704303.
257 S. Yuan, J.-S. Qin, C. T. Lollar and H.-C. Zhou, *ACS Cent. Sci.*, 2018, **4**, 440–450.
258 A. J. Howarth, Y. Liu, P. Li, Z. Li, T. C. Wang, J. T. Hupp and O. K. Farha, *Nat. Rev. Mater.*, 2016, **1**, 15018.
259 L. R. Redfern and O. K. Farha, *Chem Sci*, 2019, **10**, 10666–10679.
260 C. Healy, K. M. Patil, B. H. Wilson, L. Hermanspahn, N. C. Harvey-Reid, B. I. Howard, C. Kleinjan, J. Kolien, F. Payet, S. G. Telfer, P. E. Kruger and T. D. Bennett, *Coord. Chem. Rev.*, 2020, **419**, 213388.
261 T. Devic and C. Serre, *Chem Soc Rev*, 2014, **43**, 6097–6115.
262 J.-P. Zhang, Y.-B. Zhang, J.-B. Lin and X.-M. Chen, *Chem. Rev.*, 2012, **112**, 1001–1033.
263 N. Mosca, R. Vismara, J. A. Fernandes, G. Tuci, C. Di Nicola, K. V. Domasevitch, C. Giacobbe, G. Giambastiani, C. Pettinari, M. Aragones-Anglada, P. Z. Moghadam, D. Fairen-Jimenez, A. Rossin and S. Galli, *Chem. – Eur. J.*, 2018, **24**, 13170–13180.
264 R. Vismara, G. Tuci, A. Tombesi, K. V. Domasevitch, C. Di Nicola, G. Giambastiani, M. R. Chierotti, S. Bordignon, R. Gobetto, C. Pettinari, A. Rossin and S. Galli, *ACS Appl. Mater. Interfaces*, 2019, **11**, 26956–26969.

265 R. Vismara, G. Tuci, N. Mosca, K. V. Domasevitch, C. Di Nicola, C. Pettinari, G. Giambastiani, S. Galli and A. Rossin, *Inorg. Chem. Front.*, 2019, **6**, 533–545.
266 G. Mercuri, M. Moroni, K. V. Domasevitch, C. Di Nicola, P. Campitelli, C. Pettinari, G. Giambastiani, S. Galli and A. Rossin, *Chem. – Eur. J.*, 2021, **27**, 4746–4754.
267 K. J. Gagnon, H. P. Perry and A. Clearfield, *Chem. Rev.*, 2012, **112**, 1034–1054.
268 G. Yücesan, Y. Zorlu, M. Stricker and J. Beckmann, *Coord. Chem. Rev.*, 2018, **369**, 105–122.
269 P. Z. Moghadam, S. M. J. Rogge, A. Li, C.-M. Chow, J. Wieme, N. Moharrami, M. Aragones-Anglada, G. Conduit, D. A. Gomez-Gualdron, V. Van Speybroeck and D. Fairen-Jimenez, *Matter*, 2019, **1**, 219–234.
270 F. M. Amombo Noa, M. Abrahamsson, E. Ahlberg, O. Cheung, C. R. Göb, C. J. McKenzie and L. Öhrström, *Chem*, , DOI:10.1016/j.chempr.2021.07.006.
271 J. H. Cavka, S. Jakobsen, U. Olsbye, N. Guillou, C. Lamberti, S. Bordiga and K. P. Lillerud, *J. Am. Chem. Soc.*, 2008, **130**, 13850–13851.
272 V. Guillerm, F. Ragon, M. Dan-Hardi, T. Devic, M. Vishnuvarthan, B. Campo, A. Vimont, G. Clet, Q. Yang, G. Maurin, G. Férey, A. Vittadini, S. Gross and C. Serre, *Angew. Chem. Int. Ed.*, 2012, **51**, 9267–9271.
273 J. Rumble, *CRC Handbook of Chemistry and Physics*, CRC Press.
274 USGS National Minerals Information Center - Zirconium and Hafnium, https://pubs.usgs.gov/periodicals/mcs2021/mcs2021-zirconium-hafnium.pdf.
275 E.-S. M. El-Sayed and D. Yuan, *Green Chem*, 2020, **22**, 4082–4104.
276 J. An, S. J. Geib and N. L. Rosi, *J. Am. Chem. Soc.*, 2009, **131**, 8376–8377.
277 E. S. Grape, J. G. Flores, T. Hidalgo, E. Martínez-Ahumada, A. Gutiérrez-Alejandre, A. Hautier, D. R. Williams, M. O'Keeffe, L. Öhrström, T. Willhammar, P. Horcajada, I. A. Ibarra and A. K. Inge, *J. Am. Chem. Soc.*, 2020, **142**, 16795–16804.
278 S. Shalini, S. Nandi, A. Justin, R. Maity and R. Vaidhyanathan, *Chem. Commun.*, 2018, **54**, 13472–13490.
279 T. Wang, E. Lin, Y.-L. Peng, Y. Chen, P. Cheng and Z. Zhang, *Coord. Chem. Rev.*, 2020, **423**, 213485.
280 G. Wißmann, A. Schaate, S. Lilienthal, I. Bremer, A. M. Schneider and P. Behrens, *Microporous Mesoporous Mater.*, 2012, **152**, 64–70.
281 E. Alvarez, N. Guillou, C. Martineau, B. Bueken, B. Van de Voorde, C. Le Guillouzer, P. Fabry, F. Nouar, F. Taulelle, D. de Vos, J.-S. Chang, K. H. Cho, N. Ramsahye, T. Devic, M. Daturi, G. Maurin and C. Serre, *Angew. Chem. Int. Ed.*, 2015, **54**, 3664–3668.
282 C. Robl and A. Weiss, *Mater. Res. Bull.*, 1987, **22**, 373–380.
283 S. R. Batten and R. Robson, *Angew. Chem. Int. Ed.*, 1998, **37**, 1460–1494.
284 S. R. Batten, *CrystEngComm*, 2001, **3**, 67–72.
285 V. A. Blatov, L. Carlucci, G. Ciani and D. M. Proserpio, *CrystEngComm*, 2004, **6**, 377–395.
286 Y.-N. Gong, D.-C. Zhong and T.-B. Lu, *CrystEngComm*, 2016, **18**, 2596–2606.
287 O. Kwon, S. Park, H.-C. Zhou and J. Kim, *Chem Commun*, 2017, **53**, 1953–1956.
288 G. Verma, S. Butikofer, S. Kumar and S. Ma, *Top. Curr. Chem.*, 2019, **378**, 4.
289 S. Subramanian and M. J. Zaworotko, *Angew. Chem. Int. Ed. Engl.*, 1995, **34**, 2127–2129.
290 S. Noro, S. Kitagawa, M. Kondo and K. Seki, *Angew. Chem. Int. Ed.*, 2000, **39**, 2082–2084.

291 O. Shekhah, Y. Belmabkhout, Z. Chen, V. Guillerm, A. Cairns, K. Adil and M. Eddaoudi, *Nat. Commun.*, 2014, **5**, 4228.
292 P. M. Bhatt, Y. Belmabkhout, A. Cadiau, K. Adil, O. Shekhah, A. Shkurenko, L. J. Barbour and M. Eddaoudi, *J. Am. Chem. Soc.*, 2016, **138**, 9301–9307.
293 A. Kumar, C. Hua, D. G. Madden, D. O'Nolan, K.-J. Chen, L.-A. J. Keane, J. J. Perry and M. J. Zaworotko, *Chem Commun*, 2017, **53**, 5946–5949.
294 Y. Belmabkhout, P. M. Bhatt, K. Adil, R. S. Pillai, A. Cadiau, A. Shkurenko, G. Maurin, G. Liu, W. J. Koros and M. Eddaoudi, *Nat. Energy*, 2018, **3**, 1059–1066.
295 Z. Zhang, X. Cui, L. Yang, J. Cui, Z. Bao, Q. Yang and H. Xing, *Ind. Eng. Chem. Res.*, 2018, **57**, 7266–7274.
296 X. Cui, K. Chen, H. Xing, Q. Yang, R. Krishna, Z. Bao, H. Wu, W. Zhou, X. Dong, Y. Han, B. Li, Q. Ren, M. J. Zaworotko and B. Chen, *Science*, 2016, **353**, 141–144.
297 V. Guillerm, L. Garzón-Tovar, A. Yazdi, I. Imaz, J. Juanhuix and D. Maspoch, *Chem. – Eur. J.*, 2017, **23**, 6829–6835.
298 A. Schneemann, V. Bon, I. Schwedler, I. Senkovska, S. Kaskel and R. A. Fischer, *Chem. Soc. Rev.*, 2014, **43**, 6062–6096.
299 S. Krause, N. Hosono and S. Kitagawa, *Angew. Chem. Int. Ed.*, 2020, **59**, 15325–15341.
300 J. A. Mason, J. Oktawiec, M. K. Taylor, M. R. Hudson, J. Rodriguez, J. E. Bachman, M. I. Gonzalez, A. Cervellino, A. Guagliardi, C. M. Brown, P. L. Llewellyn, N. Masciocchi and J. R. Long, *Nature*, 2015, **527**, 357–361.
301 C. Serre, F. Millange, S. Surblé and G. Férey, *Angew. Chem. Int. Ed.*, 2004, **43**, 6285–6289.
302 C. Mellot-Draznieks, C. Serre, S. Surblé, N. Audebrand and G. Férey, *J. Am. Chem. Soc.*, 2005, **127**, 16273–16278.
303 C. Serre, C. Mellot-Draznieks, S. Surblé, N. Audebrand, Y. Filinchuk and G. Férey, *Science*, 2007, **315**, 1828–1831.
304 U. Stoeck, S. Krause, V. Bon, I. Senkovska and S. Kaskel, *Chem. Commun.*, 2012, **48**, 10841–10843.
305 S. Krause, V. Bon, I. Senkovska, U. Stoeck, D. Wallacher, D. M. Többens, S. Zander, R. S. Pillai, G. Maurin, F.-X. Coudert and S. Kaskel, *Nature*, 2016, **532**, 348–352.
306 J. D. Evans, L. Bocquet and F.-X. Coudert, *Chem*, 2016, **1**, 873–886.
307 T. Loiseau, C. Serre, C. Huguenard, G. Fink, F. Taulelle, M. Henry, T. Bataille and G. Férey, *Chem. – Eur. J.*, 2004, **10**, 1373–1382.
308 D. Li and K. Kaneko, *Chem. Phys. Lett.*, 2001, **335**, 50–56.
309 H. Kajiro, A. Kondo, K. Kaneko and H. Kanoh, *Int. J. Mol. Sci.*, , DOI:10.3390/ijms11103803.
310 D. Fairen-Jimenez, S. A. Moggach, M. T. Wharmby, P. A. Wright, S. Parsons and T. Düren, *J. Am. Chem. Soc.*, 2011, **133**, 8900–8902.
311 N. Chanut, A. Ghoufi, M.-V. Coulet, S. Bourrelly, B. Kuchta, G. Maurin and P. L. Llewellyn, *Nat. Commun.*, 2020, **11**, 1216.
312 L. Hamon, P. L. Llewellyn, T. Devic, A. Ghoufi, G. Clet, V. Guillerm, G. D. Pirngruber, G. Maurin, C. Serre, G. Driver, W. van Beek, E. Jolimaître, A. Vimont, M. Daturi and G. Férey, *J. Am. Chem. Soc.*, 2009, **131**, 17490–17499.
313 F.-X. Coudert, *Phys Chem Chem Phys*, 2010, **12**, 10904–10913.

314 G. Fraux, A. Boutin, A. H. Fuchs and F.-X. Coudert, *Adsorption*, 2018, **24**, 233–241.
315 http://www.cchem.berkeley.edu/molsim/teaching/spring2013/CCS/Group8/packed.html, http://www.cchem.berkeley.edu/molsim/teaching/spring2013/CCS/Group8/packed.html.
316 C. Zhang, L. Wang, G. Maurin and Q. Yang, *AIChE J.*, 2018, **64**, 4089–4096.
317 S. Hiraide, Y. Sakanaka, H. Kajiro, S. Kawaguchi, M. T. Miyahara and H. Tanaka, *Nat. Commun.*, 2020, **11**, 3867.
318 L. A. Darunte, T. Sen, C. Bhawanani, K. S. Walton, D. S. Sholl, M. J. Realff and C. W. Jones, *Ind. Eng. Chem. Res.*, 2019, **58**, 366–377.
319 F.-X. Coudert, *Chem. Mater.*, 2015, **27**, 1905–1916.
320 J. H. Lee, S. Jeoung, Y. G. Chung and H. R. Moon, *Coord. Chem. Rev.*, 2019, **389**, 161–188.
321 S. K. Elsaidi, M. H. Mohamed, D. Banerjee and P. K. Thallapally, *Coord. Chem. Rev.*, 2018, **358**, 125–152.
322 F. Millange and R. I. Walton, *Isr. J. Chem.*, 2018, **58**, 1019–1035.
323 I. Senkovska, F. Hoffmann, M. Fröba, J. Getzschmann, W. Böhlmann and S. Kaskel, *Microporous Mesoporous Mater.*, 2009, **122**, 93–98.
324 F. M. Amombo Noa, E. Svensson Grape, S. M. Brülls, O. Cheung, P. Malmberg, A. K. Inge, C. J. McKenzie, J. Mårtensson and L. Öhrström, *J. Am. Chem. Soc.*, 2020, **142**, 9471–9481.
325 A. Gonzalez-Nelson, F.-X. Coudert and M. A. van der Veen, *Nanomaterials*, , DOI:10.3390/nano9030330.
326 M. Witman, S. Ling, S. Jawahery, P. G. Boyd, M. Haranczyk, B. Slater and B. Smit, *J. Am. Chem. Soc.*, 2017, **139**, 5547–5557.
327 D. Banerjee, Z. Zhang, A. M. Plonka, J. Li and J. B. Parise, *Cryst. Growth Des.*, 2012, **12**, 2162–2165.
328 M. Agrawal and D. S. Sholl, *ACS Appl. Mater. Interfaces*, 2019, **11**, 31060–31068.
329 C. M. Simon, E. Braun, C. Carraro and B. Smit, *Proc. Natl. Acad. Sci.*, 2017, **114**, E287–E296.
330 P. G. Boyd, Y. Lee and B. Smit, *Nat. Rev. Mater.*, 2017, **2**, 17037.
331 C. E. Wilmer, M. Leaf, C. Y. Lee, O. K. Farha, B. G. Hauser, J. T. Hupp and R. Q. Snurr, *Nat. Chem.*, 2012, **4**, 83–89.
332 R. L. Martin and M. Haranczyk, *Cryst. Growth Des.*, 2014, **14**, 2431–2440.
333 B. J. Sikora, R. Winnegar, D. M. Proserpio and R. Q. Snurr, *Microporous Mesoporous Mater.*, 2014, **186**, 207–213.
334 Z. Yao, B. Sánchez-Lengeling, N. S. Bobbitt, B. J. Bucior, S. G. H. Kumar, S. P. Collins, T. Burns, T. K. Woo, O. K. Farha, R. Q. Snurr and A. Aspuru-Guzik, *Nat. Mach. Intell.*, 2021, **3**, 76–86.
335 X. Zhang, K. Zhang and Y. Lee, *ACS Appl. Mater. Interfaces*, 2020, **12**, 734–743.
336 D. A. Gomez-Gualdron, O. V. Gutov, V. Krungleviciute, B. Borah, J. E. Mondloch, J. T. Hupp, T. Yildirim, O. K. Farha and R. Q. Snurr, *Chem. Mater.*, 2014, **26**, 5632–5639.
337 P. G. Boyd, A. Chidambaram, E. García-Díez, C. P. Ireland, T. D. Daff, R. Bounds, A. Gładysiak, P. Schouwink, S. M. Moosavi, M. M. Maroto-Valer, J. A. Reimer, J. A. R. Navarro, T. K. Woo, S. Garcia, K. C. Stylianou and B. Smit, *Nature*, 2019, **576**, 253–256.
338 P. Müller, B. Bucior, G. Tuci, L. Luconi, J. Getzschmann, S. Kaskel, R. Q. Snurr, G. Giambastiani and A. Rossin, *Mol. Syst. Des. Eng.*, 2019, **4**, 1000–1013.

339 S. M. Moosavi, A. Nandy, K. M. Jablonka, D. Ongari, J. P. Janet, P. G. Boyd, Y. Lee, B. Smit and H. J. Kulik, *Nat. Commun.*, 2020, **11**, 4068.
340 S. P. Collins, T. D. Daff, S. S. Piotrkowski and T. K. Woo, *Sci. Adv.*, 2016, **2**, e1600954.
341 M. Witman, S. Ling, A. Gladysiak, K. C. Stylianou, B. Smit, B. Slater and M. Haranczyk, *J. Phys. Chem. C*, 2017, **121**, 1171–1181.
342 R. Anderson and D. A. Gómez-Gualdrón, *Chem. Mater.*, 2020, **32**, 8106–8119.
343 S. M. Moosavi, A. Chidambaram, L. Talirz, M. Haranczyk, K. C. Stylianou and B. Smit, *Nat. Commun.*, 2019, **10**, 539.
344 M. Yoneya, S. Tsuzuki and M. Aoyagi, *Phys. Chem. Chem. Phys.*, 2015, **17**, 8649–8652.
345 L. Kollias, D. C. Cantu, V. Glezakou, R. Rousseau and M. Salvalaglio, *Adv. Theory Simul.*, 2020, **3**, 2000092.
346 L. Kollias, D. C. Cantu, M. A. Tubbs, R. Rousseau, V.-A. Glezakou and M. Salvalaglio, *J. Am. Chem. Soc.*, 2019, **141**, 6073–6081.
347 S. A. Wells, N. F. Cessford, N. A. Seaton and T. Düren, *RSC Adv.*, 2019, **9**, 14382–14390.
348 Y. J. Colón, A. Z. Guo, L. W. Antony, K. Q. Hoffmann and J. J. de Pablo, *J. Chem. Phys.*, 2019, **150**, 104502.
349 D. Biswal and P. G. Kusalik, *J. Chem. Phys.*, 2017, **147**, 044702.
350 D. Biswal and P. G. Kusalik, *ACS Nano*, 2017, **11**, 258–268.
351 J. P. Darby, M. Arhangelskis, A. D. Katsenis, J. M. Marrett, T. Friščić and A. J. Morris, *Chem. Mater.*, 2020, **32**, 5835–5844.
352 O. T. Qazvini, R. Babarao, Z.-L. Shi, Y.-B. Zhang and S. G. Telfer, *J. Am. Chem. Soc.*, 2019, **141**, 5014–5020.
353 S. A. Bourne, A. Mondal and M. J. Zaworotko, *Cryst. Eng.*, 2001, **4**, 25–36.
354 X.-N. Cheng, W.-X. Zhang, Y.-Y. Lin, Y.-Z. Zheng and X.-M. Chen, *Adv. Mater.*, 2007, **19**, 1494–1498.
355 X.-N. Cheng, W. Xue and X.-M. Chen, *Eur. J. Inorg. Chem.*, 2010, **2010**, 3850–3855.
356 C. Livage, N. Guillou, J. Chaigneau, P. Rabu, M. Drillon and G. Férey, *Angew. Chem. Int. Ed.*, 2005, **44**, 6488–6491.
357 W.-X. Chen, G.-L. Zhuang, H.-X. Zhao, L.-S. Long, R.-B. Huang and L.-S. Zheng, *Dalton Trans.*, 2011, **40**, 10237–10241.
358 H.-N. Wang, F.-H. Liu, Y.-F. Zhu, X.-L. Wang, Z.-H. Chen and Z.-M. Su, *CrystEngComm*, 2013, **15**, 7402–7405.
359 F. Luo, J. Zheng and G. J. Long, *Cryst. Growth Des.*, 2009, **9**, 1271–1274.
360 E. Stavitski, M. Goesten, J. Juan-Alcañiz, A. Martinez-Joaristi, P. Serra-Crespo, A. V. Petukhov, J. Gascon and F. Kapteijn, *Angew. Chem. Int. Ed.*, 2011, **50**, 9624–9628.
361 M. G. Goesten, P. C. M. M. Magusin, E. A. Pidko, B. Mezari, E. J. M. Hensen, F. Kapteijn and J. Gascon, *Inorg. Chem.*, 2014, **53**, 882–887.
362 M. Taddei, J. A. van Bokhoven and M. Ranocchiari, *Inorg. Chem.*, 2020, **59**, 7860–7868.
363 C. K. Brozek, V. K. Michaelis, T.-C. Ong, L. Bellarosa, N. López, R. G. Griffin and M. Dincă, *ACS Cent. Sci.*, 2015, **1**, 252–260.
364 O. Delgado Friedrichs, M. O'Keeffe and O. M. Yaghi, *Dedic. Sten Andersson His Sci. Contrib. Solid State Struct. Chem.*, 2003, **5**, 73–78.
365 A. Schoedel, M. Li, D. Li, M. O'Keeffe and O. M. Yaghi, *Chem. Rev.*, 2016, **116**, 12466–12535.

366 T. D. Bennett, A. K. Cheetham, A. H. Fuchs and F.-X. Coudert, *Nat. Chem.*, 2017, **9**, 11–16.
367 S. Dissegna, K. Epp, W. R. Heinz, G. Kieslich and R. A. Fischer, *Adv. Mater.*, 2018, **30**, 1704501.
368 Z. Fang, B. Bueken, D. E. De Vos and R. A. Fischer, *Angew. Chem. Int. Ed.*, 2015, **54**, 7234–7254.
369 M. Taddei, *Coord. Chem. Rev.*, 2017, **343**, 1–24.
370 J. Klein, C. W. Lehmann, H.-W. Schmidt and W. F. Maier, *Angew. Chem. Int. Ed.*, 1998, **37**, 3369–3372.
371 N. Stock and T. Bein, *Angew. Chem. Int. Ed.*, 2004, **43**, 749–752.
372 P. M. Forster, N. Stock and A. K. Cheetham, *Angew. Chem. Int. Ed.*, 2005, **44**, 7608–7611.
373 N. Stock and S. Biswas, *Chem. Rev.*, 2012, **112**, 933–969.
374 B. Burger, P. M. Maffettone, V. V. Gusev, C. M. Aitchison, Y. Bai, X. Wang, X. Li, B. M. Alston, B. Li, R. Clowes, N. Rankin, B. Harris, R. S. Sprick and A. I. Cooper, *Nature*, 2020, **583**, 237–241.
375 R.-B. Lin, L. Li, A. Alsalme and B. Chen, *Small Struct.*, 2020, **1**, 2000022.
376 X. Xiong, G. Chen, S. Xiao, Y. Ouyang, H. Li and Q. Wang, *J. Phys. Chem. C*, 2020, **124**, 14603–14612.
377 L. Li, L. Guo, S. Pu, J. Wang, Q. Yang, Z. Zhang, Y. Yang, Q. Ren, S. Alnemrat and Z. Bao, *Chem. Eng. J.*, 2019, **358**, 446–455.
378 P. J. Milner, R. L. Siegelman, A. C. Forse, M. I. Gonzalez, T. Runčevski, J. D. Martell, J. A. Reimer and J. R. Long, *J. Am. Chem. Soc.*, 2017, **139**, 13541–13553.
379 R. L. Siegelman, T. M. McDonald, M. I. Gonzalez, J. D. Martell, P. J. Milner, J. A. Mason, A. H. Berger, A. S. Bhown and J. R. Long, *J. Am. Chem. Soc.*, 2017, **139**, 10526–10538.
380 E. J. Kim, R. L. Siegelman, H. Z. H. Jiang, A. C. Forse, J.-H. Lee, J. D. Martell, P. J. Milner, J. M. Falkowski, J. B. Neaton, J. A. Reimer, S. C. Weston and J. R. Long, *Science*, 2020, **369**, 392.
381 V. Y. Mao, P. J. Milner, J.-H. Lee, A. C. Forse, E. J. Kim, R. L. Siegelman, C. M. McGuirk, L. B. Porter-Zasada, J. B. Neaton, J. A. Reimer and J. R. Long, *Angew. Chem. Int. Ed.*, 2020, **59**, 19468–19477.
382 C. M. McGuirk, R. L. Siegelman, W. S. Drisdell, T. Runčevski, P. J. Milner, J. Oktawiec, L. F. Wan, G. M. Su, H. Z. H. Jiang, D. A. Reed, M. I. Gonzalez, D. Prendergast and J. R. Long, *Nat. Commun.*, 2018, **9**, 5133.
383 H. Babaei, J.-H. Lee, M. N. Dods, C. E. Wilmer and J. R. Long, *ACS Appl. Mater. Interfaces*, 2020, **12**, 44617–44621.
384 R. Hughes, G. Kotamreddy, A. Ostace, D. Bhattacharyya, R. L. Siegelman, S. T. Parker, S. A. Didas, J. R. Long, B. Omell and M. Matuszewski, *Energy Fuels*, 2021, **35**, 6040–6055.
385 L. J. Murray, M. Dinca, J. Yano, S. Chavan, S. Bordiga, C. M. Brown and J. R. Long, *J. Am. Chem. Soc.*, 2010, **132**, 7856–7857.
386 E. D. Bloch, L. J. Murray, W. L. Queen, S. Chavan, S. N. Maximoff, J. P. Bigi, R. Krishna, V. K. Peterson, F. Grandjean, G. J. Long, B. Smit, S. Bordiga, C. M. Brown and J. R. Long, *J. Am. Chem. Soc.*, 2011, **133**, 14814–14822.
387 J. W. Yoon, H. Chang, S.-J. Lee, Y. K. Hwang, D.-Y. Hong, S.-K. Lee, J. S. Lee, S. Jang, T.-U. Yoon, K. Kwac, Y. Jung, R. S. Pillai, F. Faucher, A. Vimont, M. Daturi, G. Férey, C. Serre, G. Maurin, Y.-S. Bae and J.-S. Chang, *Nat. Mater.*, 2017, **16**, 526–531.

388 D. E. Jaramillo, D. A. Reed, H. Z. H. Jiang, J. Oktawiec, M. W. Mara, A. C. Forse, D. J. Lussier, R. A. Murphy, M. Cunningham, V. Colombo, D. K. Shuh, J. A. Reimer and J. R. Long, *Nat. Mater.*, 2020, **19**, 517–521.
389 B. A. MacKay and M. D. Fryzuk, *Chem. Rev.*, 2004, **104**, 385–402.